The detrimental effect of asymmetric dimethylarginine on cholesterol efflux of macrophage foam cells

Chen, Chia-Hui; Zhao, Jin-Feng; Hsu, Chiao-Po; Kou, Yu Ru; Lu, Tse-Min; Lee, Tzong-Shyuan

Published in:
Free Radical Biology and Medicine

DOI:
10.1016/j.freeradbiomed.2019.08.016

Publication date:
2019

Document Version
Peer reviewed version

Journal Pre-proof

The detrimental effect of asymmetric dimethylarginine on cholesterol efflux of macrophage foam cells: Role of the NOX/ROS signaling

Chia-Hui Chen, Jin-Feng Zhao, Chiao-Po Hsu, Yu Ru Kou, Tse-Min Lu, Tzong-Shyuan Lee

PII: S0891-5849(19)30818-4

DOI: https://doi.org/10.1016/j.freeradbiomed.2019.08.016

Reference: FRB 14383

To appear in: *Free Radical Biology and Medicine*

Received Date: 15 May 2019

Revised Date: 7 August 2019

Accepted Date: 18 August 2019

Please cite this article as: C.-H. Chen, J.-F. Zhao, C.-P. Hsu, Y.R. Kou, T.-M. Lu, T.-S. Lee, The detrimental effect of asymmetric dimethylarginine on cholesterol efflux of macrophage foam cells: Role of the NOX/ROS signaling, *Free Radical Biology and Medicine* (2019), doi: https://doi.org/10.1016/j.freeradbiomed.2019.08.016.

Graphic abstract

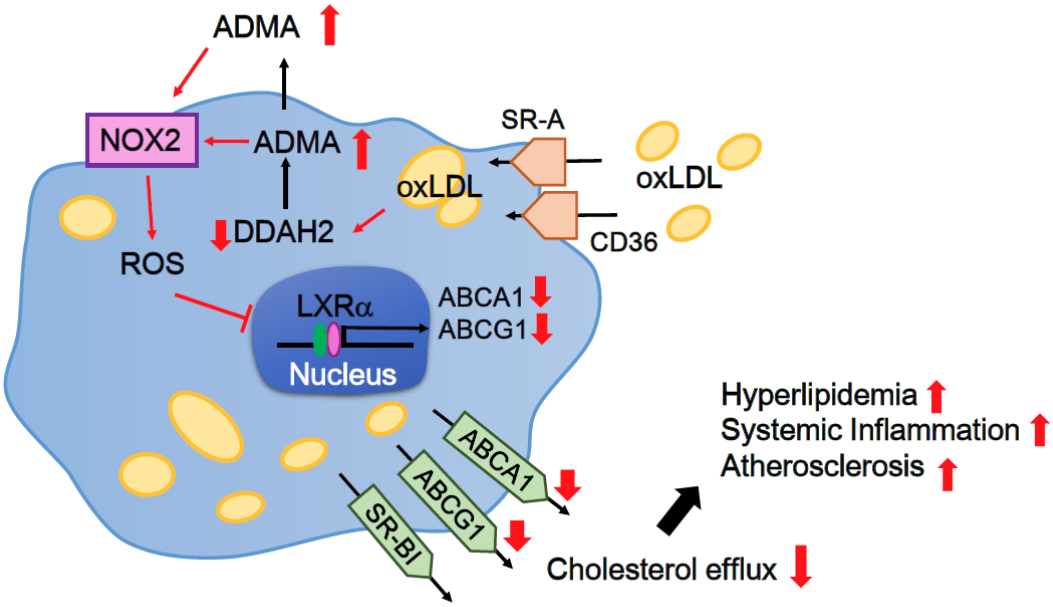

The detrimental effect of asymmetric dimethylarginine on cholesterol efflux of macrophage foam cells: Role of the NOX/ROS signaling

Chia-Hui Chen[a], Jin-Feng Zhao[b], Chiao-Po Hsu[c,d], Yu Ru Kou[a], Tse-Min Lu[c,e#], Tzong-Shyuan Lee[f#]

[a]Department of Physiology, School of Medicine, National Yang-Ming University, Taipei, Taiwan; [b]MRC Protein Phosphorylation and Ubiquitylation Unit, University of Dundee, Dundee, UK; [c]Faculty of Medicine, School of Medicine, National Yang-Ming University, Taipei, Taiwan; [d]Division of Cardiovascular Surgery, Department of Surgery, Taipei Veterans General Hospital, Taipei, Taiwan; [e]Division of Cardiology, Department of Internal Medicine, Taipei Veterans General Hospital, Taipei, Taiwan; [f]Graduate Institute and Department of Physiology, College of Medicine, National Taiwan University, Taipei, Taiwan

Short title: ADMA deregulates cholesterol metabolism in macrophages

[#]Address for reprint requests and correspondence:

Dr. Tzong-Shyuan Lee, DVM, PhD, Graduate Institute and Department of Physiology College of Medicine, National Taiwan University, Taipei 10051, Taiwan; Tel: +886-2-23123456, ext. 88242; Fax: +886-2-2396-4350, E-mail: ntutslee@ntu.edu.tw

Dr. Tse-Min Lu, MD, PhD, Division of Cardiology, Department of Internal Medicine, Taipei Veterans General Hospital, Taipei 11221, Taiwan; Tel: +886-2-28757511, Fax: +886-2-28753580, E-mail: tmlu@vghtpe.gov.tw

Abstract

Background: Asymmetric dimethylarginine (ADMA) is an endogenous nitric oxide synthase inhibitor and has been proposed to be an independent risk factor for cardiovascular diseases. However, little is known about its role in the regulation of lipid metabolism. In this study, we investigated the effect of ADMA on cholesterol metabolism and its underlying molecular mechanism.

Methods: Oxidized low-density lipoprotein (oxLDL)-induced macrophage foam cells were used as an *in vitro* model. Apolipoprotein E-deficient (apoE$^{-/-}$) hyperlipidemic mice were used as an *in vivo* model. Western blot analysis was used to evaluate protein expression. Luciferase reporter assays were used to assess the activity of promoters and transcription factors. Conventional assay kits were used to measure the levels of ADMA, cholesterol, triglycerides, and cytokines**.**

Results: Treatment with oxLDL decreased the protein expression of dimethylarginine dimethylaminohydrolase-2 (DDAH-2) but not DDAH-1. Incubation with ADMA markedly increased oxLDL-induced lipid accumulation in macrophages. ADMA impaired cholesterol efflux following oxLDL challenge and downregulated the expression of ATP-binding cassette transporter A1 (ABCA1) and ABCG1 by interfering with liver X receptor α (LXRα) expression and activity. Additionally, this inhibitory effect of ADMA on cholesterol metabolism was mediated through the activation of the NADPH oxidase/reactive oxygen species pathway. *In vivo* experiments revealed that chronic administration of ADMA for 4 weeks exacerbated systemic inflammation, decreased the aortic protein levels of ABCA1 and ABCG1, and impaired the capacity of reverse cholesterol transport, ultimately, leading to the progression of atherosclerosis in apoE$^{-/-}$ mice.

Conclusion: Our findings suggest that the ADMA/DDAH-2 axis plays a crucial role

in regulating cholesterol metabolism in macrophage foam cells and atherosclerotic progression.

***Keywords*:** asymmetric dimethylarginine; macrophage foam cell; cholesterol metabolism; ATP-binding cassette transporter; liver X receptor α; atherosclerosis

Abbreviations:

ADMA, asymmetric dimethylarginine; oxLDL, oxidized low-density lipoprotein; DDAH-1, dimethylarginine dimethylaminohydrolase-1; DDAH-2, dimethylarginine dimethylaminohydrolase-2; NBD-cholesterol, 4-nitrobenzo-2-oxa-1,3-diazole-labeled cholesterol; Dil-oxLDL, 1,1'-dioctadecyl-3,3,3',3'-tetramethylindocarbocyanine perchlorate-labeled low-density lipoprotein; apoE, apolipoprotein E; ABCA1, ATP-binding cassette transporter A1; ABCG1, ATP-binding cassette transporter G1; LXRα, liver X receptor α; NOX, NADPH oxidase; ROS, reactive oxygen species; EC, endothelial cells; eNOS, endothelial nitric oxide synthase; CAD, coronary artery disease; apoAI, apolipoprotein AI; HDL, high-density lipoprotein; RCT, reverse cholesterol transport; NAC, N-acetylcysteine; APO, apocynin; DHE, dihydroethidine; DCFH-DA, 2′,7′-dichlorofluorescin diacetate; LXRE, LXRα responsive element; Adv, adenovirus; MOI, multiplicity of infection

1. Introduction

Asymmetric dimethylarginine (ADMA) is generated from the degradation of methylated proteins and can be metabolized to citrulline by dimethylarginine dimethylaminohydrolase-1 (DDAH-1) or DDAH-2 [1]. DDAH-1 is abundant in the kidney and liver, whereas DDAH-2 expression can be detected in endothelial cells (ECs) and immune cells [1,2]. ADMA is now characterized as a circulating endogenous inhibitor of endothelial nitric oxide synthase (eNOS) [1,3]. Elevated plasma ADMA levels have been observed in patients with various risk factors for coronary artery disease (CAD), including hypercholesterolemia, atherosclerosis, hypertension, diabetes, insulin resistance, hypertriglyceridemia, and hyperhomocysteinemia [4-10]. Moreover, several studies have demonstrated that the plasma ADMA level may predict cardiovascular events and mortality in patients with CAD, renal failure, and advanced peripheral artery diseases [11,12]. During the past decades, most studies on the DDAH/ADMA system have investigated its role in the regulation of eNOS activity in ECs. However, there has been little research on the role of ADMA in the pathophysiology of macrophages.

It is well established that deregulation of cholesterol metabolism is the most critical factor for the initiation and development of atherosclerosis [13]. Excessive cholesterol deposition and persistent inflammation within the artery wall are two key hallmarks of atherosclerosis [13,14]. Both macrophage-mediated cholesterol clearance and pro-inflammatory cytokine secretion are crucial steps in the initiation and progression of atherosclerosis [13,15]. Particularly, excessive cholesterol accumulation in macrophages is mainly due to their uncontrolled uptake of oxidized low-density lipoprotein (oxLDL) or impaired cholesterol efflux [16-19]. Scavenger receptors (SRs) are responsible for internalizing oxLDL [17,18]. In contrast, the

efflux of intracellular cholesterol to apolipoprotein AI (apoAI) or high-density lipoprotein (HDL) is mediated through reverse cholesterol transport (RCT) [16,19]. Thus, moderating the expression of SRs and factors involved in RCT represents a possible therapeutic strategy for treating or preventing atherosclerosis [17,20-23]. However, less is known about the interlocking biology of ADMA and macrophages. Further investigations to delineate the role and molecular mechanisms of ADMA in the cholesterol metabolism of macrophage foam cells are warranted.

In this study, first, we investigated the role of ADMA in oxLDL-induced foam cell formation, and second, we determined whether ADMA affects the expression of SRs and factors involved in RCT and the underlying molecular mechanisms. Our third aim was to explore the effect of ADMA on the development of atherosclerosis in apolipoprotein E-deficient ($apoE^{-/-}$) mice. Here, we found that treatment with ADMA worsened the oxLDL-induced lipid accumulation of macrophage foam cells by decreasing ABC transporter-dependent cholesterol efflux. This detrimental effect of ADMA was attributed to a decrease in oxLDL-elicited LXRα activation. The *in vivo* response to ADMA may involve it modulating hyperlipidemia and systemic inflammation, as well as RCT, thus accelerating atherosclerosis progression. Our findings provide a novel explanation for the pro-atherogenic action of ADMA and suggest a potential molecular target for the treatment or prevention of atherosclerosis in the future.

2. Materials and methods

2.1. Reagents

Goat anti-SR-A antibody (Ab), rabbit anti-CD36, anti-ABCG1, anti-DDAH-1,

anti-DDAH-2 Ab, control small interfering RNA (siRNA) and NADPH oxidase 2 (NOX2) siRNA were obtained from Santa Cruz Biotechnology (Santa Cruz, CA, USA). Mouse anti-ABCA1 Ab and rabbit anti-SR-BI Ab were purchased from Abcam (Cambridge, MA, USA). ADMA, Tri reagent, mouse anti-α-tubulin Ab, human apoAI, human HDL, human LDL, N-acetylcysteine (NAC), and apocynin (APO) were purchased from Sigma Chemical (St. Louis, MO, USA). The ADMA ELISA kit was obtained from Enzo Life Sciences (Farmingdale, NY, USA). Dil-labeled LDL or oxLDL was purchased from Biomedical Technologies (Stoughton, MA, USA). The cholesterol and triglyceride assay kits were obtained from Randox (Antrim, UK). 3-hexanoyl-NBD-cholesterol was purchased from Cayman Chemical (Ann Arbor, MI, USA). TurboFect^{TM} reagent was obtained from Fermentas (Glen Burnie, MD, USA). Dihydroethidine (DHE) and 2′,7′-dichlorofluorescin diacetate (DCFH-DA) were purchased from Molecular Probes (Eugene OR, USA). The EnzyChrom $NADP^+$/NAD(P)H assay kit was obtained from BioAssay Systems (Hayward, CA, USA). ELISA kits for pro-inflammatory cytokines were purchased from R&D (Minneapolis, MN, USA).

2.2. Cell culture

Murine J774.A1 macrophages (ATCC, TIB-67) were cultured in RPMI 1640 medium supplemented with 10% fetal bovine serum (FBS), penicillin (100 U/ml), and streptomycin (100 μg/ml). Human monocytic cell line THP-1 cells (Bioresource Collection and Research Center; Hsinchu, Taiwan) were cultured in RPMI 1640 medium supplemented with 10% FBS, penicillin (100 U/ml) and streptomycin (100 μg/ml). THP-1 cells were induced with 50 nM PMA for 5 d to differentiate into macrophages.

2.3. Modification of low-density lipoprotein

oxLDL was prepared as described previously [22]. LDL was exposed to 5 μM $CuSO_4$ for 24 h at 37 °C, and Cu^{2+} was then removed by extensive dialysis. The extent of modification was determined by measuring thiobarbituric acid-reactive substances (TBARs). OxLDL containing approximately 30-60 nmol TBARs defined as malondialdehyde equivalent per milligram LDL protein was used for experiments. HOCL-oxLDL was prepared by adding 1 mmol/L (Final concentration) NaOCl into LDL or Dil-LDL solutions (1 mg/mL) at 37◦C for 40 min, and HOCl was then removed by extensive dialysis.

2.4. Oil red O staining

Cells were fixed with 4% paraformaldehyde and then stained with 0.5% Oil red O. Hematoxylin was used for counterstaining.

2.5. Quantitative real-time PCR (qRT-PCR)

Total RNA was isolated from cells using Tri reagent and then converted into cDNA by reverse transcriptase (Fermentas Glen Burnie, MD, USA) with oligo-dT primers. The obtained cDNAs were then used as the templates for qRT-PCR. The qRT-PCR reaction was performed using the TaqMan® probe-based real-time quantification system (Foster, CA). The relative amount of mRNAs was calculated with glyceraldehyde 3-phosphate dehydrogenase (GAPDH) mRNA as the invariant control.

2.6. Preparation of nuclear extracts

Nuclear extracts were prepared as described previously [22]. Cells were lysed in 10 mM HEPES (pH 7.9), 10 mM KCl, 1.5 mM $MgCl_2$, 0.5% Nonidet P-40, 1 μg/ml leupeptin, 10 μg/ml aprotinin, and 1 mM phenylmethylsulfonyl fluoride. Nuclei were pelleted at 5000 × *g* for 5 min at 4 °C, and the resulting supernatants were used as the cytosolic fraction. Nuclei were resuspended in 50 mM Tris (pH 7.5), 300 mM NaCl,

1% Triton X-100, 5 mM ethylenediaminetetraacetate, 1 μg/ml leupeptin, 10 μg/ml aprotinin, and 1 mM phenylmethylsulfonyl fluoride and incubated on ice for 5 min. After centrifugation at 12,000 × *g* for 5 min at 4 °C, the supernatant was collected as the nuclear extract.

2.7. Western blot analysis

Cells or tissues were lysed with PBS containing 1% Triton X-100, 0.1% SDS, 0.5% sodium deoxycholate, 1 μg/ml leupeptin, 10 μg/ml aprotinin, and 1 mM PMSF on ice. After sonication, crude extracts underwent centrifugation at 12000 × *g* for 5 min at 4 °C. The supernatants were collected as cell lysates. All protein concentrations were determined by a protein assay. Aliquots (50 μg) of cell lysates were separated using 8% SDS-PAGE and then transblotted on an Immobilon^{TM}-P membrane (Millipore, Bedford, MA). After blocking with 5% skim milk, blots were incubated with primary Abs and then secondary Abs. The protein bands were detected with an enhanced chemiluminescence kit (PerkinElmer, Boston, MA) and quantified using ImageQuant 5.2 software (Healthcare Bio-Sciences, PA).

2.8. Cholesterol and triglyceride measurements

Cellular cholesterol and triglycerides were extracted using hexane/isopropanol (3/2, v/v). The extracts were dried, and the reagent from the assay kit was then added to measure the levels of cholesterol and triglycerides.

2.9. Dil-oxLDL binding assay

The assay was performed as described previously [22]. Macrophages were treated with various concentration of ADMA (0, 0.25, 0.5, 1.0 μg/ml) for 12 h and then with 10 μg/ml Dil-oxLDL at 4 °C for 4 h. Cells were washed, and lysates were analyzed using fluorometry (Molecular Devices) with a 514-nm excitation laser line and 550-nm emission filters.

2.10. Cholesterol efflux assay

The assay was performed as described previously [22]. Macrophages were treated with various concentrations of ADMA (0, 0.25, 0.5, 1.0 μg/ml) for 12 h and then equilibrated with NBD-cholesterol (1 μg/ml) for an additional 6 h in the presence of apoAI (10 μg/ml) or HDL (50 μg/ml) with or without ADMA. NBD-cholesterol-labeled cells were washed with PBS and incubated in RPMI 1640 medium for 6 h. The fluorescence-labeled cholesterol released from the cells into the medium was measured using a multilabel counter (PerkinElmer, Waltham, MA). *In vivo* cholesterol efflux was determined as described previously with modifications [24]. Briefly, after removing the apoB-containing lipoproteins from mouse plasma, the supernatant, as the high-density lipoprotein fraction, was diluted to 2.8% (equivalent to 2% serum) in culture medium. Cholesterol efflux was measured as the difference in the release of fluorescence-labeled cholesterol from vehicle- or TO901317-treated macrophages.

2. 11. Transient transfection and luciferase reporter assay

Cells were transfected with the plasmids phABCA1 (-928)-Luc, a reporter plasmid for the human ABCA1 promoter, phABCA1-DR4m-Luc, a reporter plasmid with a mutation in the LXRα responsive element (LXRE) (kindly provided by Dr. A.R. Tall, Division of Molecular Medicine, Department of Medicine, Columbia University, New York, NY, USA) or in LXR/RXR ligand binding systems, pM-hLXRα or pM-hRXRα, respectively, and with pG5SEAP using TurboFect^{TM}. The ligand binding domains of hLXRα and hRXRα were isolated from pENTR221-NR1H3 and pENTR221-NR1H2, respectively (Addgene, Watertown, MA, USA) and subcloned into the pM vector (Clontech, Mountain View, CA) using *Mlu*I and *Xba*I. The pGL3-renilla plasmid was cotransfected as a transfection control. After transfection for 24 h, cells were treated

with TO-901317 for another 18 h. The cells were then lysed for luciferase (Luc) and renilla activity assays. For siRNA transfection, macrophages were transfected with control siRNA or NOX2 siRNA with use of Lipofectamine for 24 h for the indicated experiments.

2.12. Measurement of intracellular ROS levels

Macrophages were washed with PBS and incubated in cell medium containing 10 μM HE or 20 μM DCFH-DA at 37 °C for 30 min. Subsequently, the cell medium containing DHE or DCFH-DA was removed and replaced with fresh medium. Cells were then incubated with ADMA (0.5 μg/ml) for 0-30 min. Cells were washed twice with PBS and detached with trypsin/EDTA, and fluorescence intensity was analyzed using FACScan flow cytometry (Becton Dickinson, San Jose, CA, USA) at 530 nm excitation and 620 nm emission for ethidium (ETH) and 488 nm excitation and 530 nm emission for DCF.

2.13. Determination of NADPH oxidase activity

Macrophages were incubated with ADMA (0.5 μg/ml) for different times or in the absence or the presence of NAC (10 mM) or APO (50 μM) for 15 min. The activity of NOX was analyzed using the EnzyChrom $NADP^+$/NADPH assay kit**.**

2.14. Adenoviral construction and infection

A replication-defective recombinant adenoviral vector containing a human phosphoglycerate kinase (hPGK) promoter driving the human DDAH-2 (Adv-DDAH-2), as well as hPGK alone to serve as a control (Adv-null), were generated by homologous recombination according to the protocol provided (Clontech, Palo Alto, CA) and amplified in HEK293 cells, purified by CsCl ultracentrifugation, and stored in 10 mm Tris-HCl (pH 7.4), 1 mm MgCl2, and 10% (vol/vol) glycerol in liquid nitrogen until used for experiments. The titers of

adenovirus were determined by plaque assay in HEK293 cells. Macrophages were infected with Ad at multiplicity of infection (MOI) of 12.5-50 for 24 h and then subjected to experiments.

2.15. Animals

All animal experiments were approved by the Animal Care and Utilization Committee of National Yang-Ming University (No. 990803). Male apoE$^{-/-}$ mice (Jackson Laboratory, Bar Harbor, Maine) (4 months old) were fed a chow diet, which contained 4.5% fat by weight (0.02% cholesterol) (Newco Distributors, Redwood, CA) and maintained under conventional housing conditions. Mice received a daily intraperitoneal (i.p.) injection of ADMA (5 mg/kg, n=10) or saline (vehicle control, n=10) for 4 weeks. At the end of the experiments, mice were euthanized with CO_2. Serum, hearts, and aortas were collected for blood biochemistry, histology, and western blot analyses.

2.16. Histological assessment

Harvested hearts were fixed and embedded in paraffin. Heart tissue blocks were serially sectioned at 8 μm. For the quantification of atherosclerotic lesions, 50 serial sections from the aortic sinus of each mouse were collected. A total of 10 sections sampled from every 5 consecutive sections were deparaffinized and subjected to H&E staining. The photomicrographs of lesions at aortic root were taken under a Motic TYPE 102M microscope (Motic Images Plus 2.0, China). The lesion size was then calculated from the average of the area quantified from the 10 sections by use of a computer imaging software (Motic Images Plus 2.0, China).

2.17. Serum lipid profile analysis

Serum was collected from experimental mice. The serum levels of total cholesterol and triglycerides were measured using Spotchem EZ SP 4430 (ARKRAY,

Inc., Kyoto, Japan).

2.18. Measurement of inflammatory cytokines

The concentrations of pro-inflammatory cytokines, including tumor necrosis factor (TNF)-α, interleukin (IL)-1β, IL-6, monocyte chemoattractant protein-1 (MCP-1), and macrophage inflammatory protein-2 (MIP-2) in serum were measured using ELISA kits according to the manufacturer's instructions.

2.19. Statistical analysis

Results are presented as the mean ± standard error of the mean (SEM) from 5 independent experiments or 10 mice. The Mann-Whitney test was used to compare two independent groups. The Kruskal-Wallis test followed by the Bonferroni post hoc analyses was performed to test multiple groups. SPSS v8.0 (SPSS Inc, Chicago, IL) was used for analyses. A difference was considered statistically significant when $p < 0.05$.

3. Results

3.1. DDAH-2 is involved in the formation of macrophage foam cells

We first investigated the distribution of DDAHs in aortas from hyperlipidemic apoE$^{-/-}$ mice. The expression of DDAH-1 and DDAH-2 was mainly confined to macrophage foam cells of atherosclerotic lesions (Fig. 1A). Modified LDL, in particular oxLDL, deregulates the cholesterol metabolism of macrophages, leading to the formation of foam cells and progression of atherosclerosis [13,15]. We thus determined whether oxLDL affects the expression of DDAH-2 in macrophages. We found that incubation with oxLDL dose-dependently decreased the protein expression of DDAH-2 but not DDAH-1 in macrophages (Fig. 1B). In addition, oxLDL increased the intracellular level of ADMA (Fig. 1C). Similar results were observed in human

THP-1-derived macrophages (Fig. 1D and E). Furthermore, treatment with ADMA increased oxLDL-induced lipid accumulation in macrophages (Fig. 2A-D). Similar to the results that found in murine macrophages, ADMA also exacerbated the oxLDL-induced lipid accumulation in human THP-1-derived macrophages (Fig. 2E and F). Moreover, ADMA aggravated HOCl-oxLDL-induced lipid accumulation in murine macrophages (Supplementary Fig. S1). These findings suggest that the DDAH-2/ADMA system may play a role in the regulation of lipid metabolism during the transformation of macrophage foam cells.

3.2. ADMA interferes with oxLDL-induced ABC transporter-dependent cholesterol efflux in macrophages

We delineated the mechanisms underlying the detrimental effect of ADMA on the formation of foam cells by determining the effect of ADMA on the regulation of cholesterol homeostasis and the expression of SRs and RCTs in murine J774.A1 macrophages or human THP-1 derived macrophages. Treatment with ADMA did not affect Dil-oxLDL binding and the protein expression of scavenger receptors, including SR-A and CD36 (Fig. 3A-F). In contrast, treatment with ADMA significantly decreased the apoAI- or HDL-dependent cholesterol efflux in macrophages (Fig. 4A, B, D and E). Additionally, treating macrophages with ADMA decreased the oxLDL-induced increase in protein levels of ABCA1 and ABCG1 without affecting the protein expression of SR-BI (Fig. 4C and F). These results suggest that ADMA exacerbates oxLDL-induced lipid accumulation in foam cells by interfering with ABC transporter-dependent cholesterol efflux.

3.3. ADMA impairs oxLDL-mediated LXRα activation

Furthermore, treatment with ADMA decreased the oxLDL-induced mRNA expression of ABCA1 and ABCG1, as revealed by RT-PCR (Fig. 5A), suggesting that

ADMA may modulate the expression of ABCA1 and ABCG1 through transcriptional regulation. To determine whether the key transcription factor LXRα is involved in ADMA-mediated downregulation of ABCA1 and ABCG1, we examined the effect of ADMA on the expression and activity of LXRα in macrophages. As shown in Fig. 5B, ADMA decreased the nuclear levels of LXRα elicited by oxLDL. Additionally, we found that treatment with ADMA decreased LXRα activity induced by oxLDL (Fig. 5C). Similarly, treatment with ADMA also reduced the LXRα activity induced by the LXRα agonist TO901317 (Fig. 5C). These results indicate that the deregulation of LXRα activation is a crucial event in the ADMA-mediated exacerbation of lipid accumulation in foam cells.

3.4. Overexpression of DDAH-2 abolishes the ADMA-induced impairment of cholesterol efflux and exacerbation of lipid accumulation in macrophages

DDAH-2 plays a crucial role in regulating ADMA metabolism in macrophages [25]. We determined whether overexpression of DDAH-2 protects against the unfavorable effects of ADMA on cholesterol metabolism. Infection with Ad-DDAH-2 dose-dependently increased DDAH-2 expression (Fig. 6A) and rescued ADMA-impaired apoAI- and HDL-dependent cholesterol efflux (Fig. 6B and C). However, Adv-null had no such an effect (data not shown) on cholesterol efflux by ADMA. In addition, overexpression of DDAH-2 decreased the ADMA-induced increase in lipid accumulation following incubation with Dil-oxLDL (Fig. 6D and E). These results suggest that DDAH plays a protective role in the deregulation of lipid metabolism in macrophage foam cells.

3.5. ADMA impairs cholesterol efflux by activating the NOX-ROS signaling pathway

We then determined the molecular mechanism by which ADMA interferes with

cholesterol efflux in macrophages. The NOX-ROS signaling pathway has been reported to be involved in the detrimental effects of ADMA [26]. Our results demonstrated that ADMA (0.5 μg/ml) increased NOX activity as early as 2 min, with a peak level at 15 min (Fig. 7A). In addition, ROS production was increased with ADMA treatment as early as 5 min, with a peak level at 15 min (Fig. 7B-E). Pretreatment with the NOX inhibitor APO or antioxidant NAC abrogated the ADMA-induced increase in ROS production (Fig. 8A and B). To provide further evidence that the ROS-NOX signaling pathway is crucial in the ADMA-induced decrease in cholesterol efflux and increase in lipid accumulation, we depleted NOX activity or ROS production by treatment with APO or NAC, respectively. Our results showed that the detrimental effects of ADMA on cholesterol efflux and lipid accumulation were blunted with APO or NAC (Fig. 8C-F). Moreover, transfection with NOX2 siRNA prevented the detrimental effects of ADMA on ROS production (Fig. 8G and H) and oxLDL-mediated lipid accumulation (Fig. 8I and J). Thus, the ROS-NOX signaling pathway plays a crucial role in regulating the ADMA-mediated impairment of cholesterol metabolism in macrophages.

3.6. ADMA administration impairs the capacity for RCT, aggravates systemic inflammation, and accelerates the progression of atherosclerosis in apoE$^{-/-}$ mice

To confirm the *in vitro* findings, we used hyperlipidemic apoE$^{-/-}$ mice as an *in vivo* model to delineate the potential functional significance of ADMA in cholesterol metabolism, systemic inflammation, and atherosclerosis. Chronic administration of ADMA for 4 weeks increased the serum levels of ADMA (ADMA-treated group vs. vehicle-treated group = 2.17 ± 0.40 μmol/L vs. 1.11 ± 0.26 μmol/L) but did not alter the body weight (ADMA-treated group vs. vehicle-treated group = 28.2 ± 2.1 g vs. 27.8 ± 1.6 g). Histological examinations revealed that the size of atherosclerotic

lesions that developed in ADMA-treated apoE$^{-/-}$ mice was significantly greater than those found in vehicle-treated apoE$^{-/-}$ mice (Fig. 9A). Serum levels of total cholesterol, non-HDL-c, HDL-c and triglycerides were significantly increased in ADMA-treated apoE$^{-/-}$ mice (Fig. 9B). Furthermore, ADMA decreased the protein levels of LXRα, ABCA1, and ABCG1 in the aortas of apoE$^{-/-}$ mice without affecting the protein levels of SR-A, CD36, and SR-BI (Fig. 9C). The capacity for serum cholesterol reverse transport was significantly lower in ADMA-treated apoE$^{-/-}$ than in vehicle-treated apoE$^{-/-}$ mice (Fig. 9D). Moreover, treatment with ADMA exacerbated systemic inflammation as evidenced by elevated serum levels of TNF-α, IL-1β, IL-6, MCP-1, and MIP-2 (Fig. 9E). Collectively, these findings suggest that ADMA might be an important factor in the deregulation of cholesterol metabolism and systemic inflammation, as well as the progression of atherosclerosis *in vivo* (Fig. 10).

4. Discussion

In this study, we found that ADMA has a detrimental effect on cholesterol homeostasis during the transformation of macrophage foam cells. We first confirmed that the expression of DDAH-1 and DDAH-2 was mainly localized in macrophage foam cells. Furthermore, we demonstrated that oxLDL, the most critical atherogenic factor, downregulated the expression of DDAH-2 and consequently increased the intracellular level of ADMA. We also found that ADMA augmented oxLDL-induced lipid accumulation in macrophages. In addition, treatment with ADMA impaired cholesterol efflux, as well as the expression of LXRα, ABCA1, and ABCG1 following oxLDL treatment. Moreover, ADMA markedly increased NOX activity and ROS production. These detrimental effects of ADMA on ABC transporter-dependent cholesterol efflux and lipid accumulation were blunted by treatment with the ROS

scavenger NAC or NOX inhibitor APO or overexpression of DDAH-2. Finally, *in vivo*, administration of ADMA worsened aortic inflammation and deregulation of cholesterol metabolism and ultimately resulted in the progression of atherosclerosis in apoE$^{-/-}$ mice. This inhibitory effect of ADMA on cellular function is consistent with our previous report in which we found that ADMA abolishes the effects of the lipid-lowering drug simvastatin on phosphorylation of endothelial nitric oxide synthase (eNOS), NO production, and angiogenesis as well as the clinical benefits of statins [26]. Thus, our findings suggest that ADMA interferes with the lipid metabolism of macrophage foam cells by deregulating cholesterol clearance. Collectively, we provide the new evidence to support the pro-atherogenic role of ADMA in the transformation of foam cells and the development of atherosclerosis.

Regarding to the relevance of the levels of ADMA added *in vitro* studies, we believe that the concentration of exogenous ADMA (0.5 μmol/L) used in this study is clinically relevant. Our previous study demonstrated that the circulating level of ADMA in CAD patients was about ~0.5 μmol/L [26]. Moreover, a meta-analysis study demonstrated the plasma levels of ADMA in CAD patients were range from 0.345±0.178 to 3.43±0.57 μmol/L [27], suggesting the serum levels of ADMA in apoE$^{-/-}$ mice with or without ADMA administration of daily i.p. injection at 5 mg/kg (ADMA-treated group vs. vehicle-treated group = 2.17 ± 0.40 μmol/L vs. 1.11 ± 0.26 μmol/L) were related that in CAD patients.

The accumulation of macrophage foam cells in the intima of the aorta is a key event in the initiation and progression of atherosclerosis [28]. RCT is a crucial regulatory mechanism for cholesterol clearance from the human body [29]. ABCA1 and ABCG1 are the key players in this process [30,31]. Increased expression of ABCA1 or ABCG1 in macrophages promotes cholesterol efflux and decreases

cholesterol accumulation in foam cells, thereby slowing the progression of atherosclerosis [23,31-33]. In contrast, loss of ABCA1 or ABCG1 function impairs RCT and results in cholesterol accumulation in foam cells, leading to the acceleration of atherosclerosis [34,35]. Our current findings further confirmed this notion by providing evidence that ADMA decreased the expression of ABCA1 and ABCG1 and impaired RCT, leading to an increase in intracellular cholesterol accumulation in macrophages following oxLDL challenge. In view of their function, the downregulation of both ABCA1 and ABCG1 by ADMA observed in this study is likely to decrease cholesterol metabolism and promote foam cell formation. Notably, intralesional macrophage-mediated pro-inflammatory mediator secretion also plays a crucial role in the progression of atherosclerosis [36,37]. Deregulation of the DDAH-ADMA system has been reported to be involved in the pathogenesis of sepsis and metabolic diseases [38-40]. Several lines of evidence indicate that treatment with ADMA upregulates the expression of pro-inflammatory mediators, including IL-8, inducible NOS, and macrophage migration inhibitory factor in macrophages [41,42]. Indeed, our *in vivo* results further confirmed this, as chronic treatment with ADMA for 4 weeks increased the levels of TNF-α, IL-1β, IL-6, MCP-1, and MIP-2 in the sera of *apoE*$^{-/-}$ mice.

NOX-derived ROS is an essential secondary messenger for regulating cellular functions and the progression of cardiovascular diseases [43]. In the initial stage of cardiovascular diseases, NOX-ROS signaling-elicited oxidative stress deregulates intracellular signaling cascades and cellular functions and leads to disease progression [44,45]. Targeting NOX-ROS signaling with antioxidants has been shown to be a successful and potential therapeutic strategy for preventing oxidative stress-induced pro-atherogenic events in clinical trials and experimental studies [21,46,47]. Growing

lines of evidence suggest that the NOX-ROS signaling pathway contributes to the ADMA-mediated pathological effects [41,48,49], so activation of this pathway might be required for the detrimental effects of ADMA on cholesterol metabolism in macrophage foam cells. Indeed, our findings that treatment with NAC or APO abrogated the ADMA-mediated deregulation of cholesterol metabolism in macrophages agree with our previous findings that ADMA abolished the beneficial effects of simvastatin by triggering NOX-ROS signaling [26].

In addition to it inhibiting the ADMA-mediated activation of NOX-ROS signaling, we found that increasing the metabolic rate of ADMA by overexpressing DDAH-2 abrogated the ADMA-elicited activation of NOX-ROS signaling and thus prevented its detrimental effects on cholesterol metabolism in macrophage foam cells, which agrees with the findings reported by Jacobi et al. who found that overexpression of DDAH-1 lowers ADMA levels and ameliorates atherosclerosis in apoE$^{-/-}$ mice [50]. Moreover, we previously reported that the endothelium-specific overexpression of DDAH-2 prevents ADMA-induced interference with statin-mediated NO production and related endothelial functions [26]. Conceivably, these findings suggest that targeting ADMA represents a possible strategy for preventing the deregulation of cholesterol metabolism and the progression of atherosclerosis. Nevertheless, determining whether antioxidant therapy can prevent the ADMA-mediated detrimental effects on cholesterol metabolism and atherosclerosis requires further investigations and clinical trials.

We also showed that ADMA downregulated the expression of LXRα, the major transcriptional factor for the expression of ABCA1 and ABCG1, in ADMA-treated macrophages and apoE$^{-/-}$ mice [51,52]. LXRα is a cholesterol-sensing nuclear receptor and plays a crucial role in regulating cholesterol homeostasis in macrophages

and the pathogenesis of atherosclerosis [53]. It has been reported that activation of LXRα ameliorates lipid accumulation in macrophage foam cells and slows the progression of atherosclerosis [54,55]. Thus, our finding that ADMA downregulated LXRα, ABCA1, and ABCG1; impaired cholesterol efflux; and promoted the progression of atherosclerosis is not surprising. Apart from the anti-atherogenic effect on lipid metabolism, LXRα was recently found to play roles in the regulation of the inflammatory response [56,57]. As such, the anti-inflammatory property of LXRα activation has been documented in viral infections, inflammatory diseases, and the above-mentioned cardiometabolic disorders in basic science studies [58-60]. Activation of LXRα by agonists downregulates the expression of inflammatory genes through a trans-repression process [61,62]. Our current finding further confirmed the anti-inflammatory effect of LXRα as evidenced by the downregulation of LXRα and increased inflammatory response within atherosclerotic lesions in ADMA-treated apoE$^{-/-}$ mice compared to those in vehicle-treated apoE$^{-/-}$ mice. Regarding the interaction between LXRα and NOX-ROS signaling, most studies on LXRα demonstrated that activation of LXRα by agonists protects cells from ROS-mediated injury or inflammation [63,64]; however, we do not have evidence to support the effect of ROS on LXRα activation and the underlying mechanism. Thus, additional studies to delineate the effect of NOX-ROS signaling on LXRα-mediated cardiovascular benefits are warranted.

However, our study contains several limitations. Our *in vitro* experiments employed the mouse macrophage J774.A1 cell line and human THP-1 cell line. It is important to confirm the implication of ADMA in cholesterol metabolism of macrophages by using primary human monocyte-derived macrophages. We did not investigate the effects of ADMA on lipid metabolism in primary human

monocyte-derived macrophages in this study for the reason that our labs are not certified to perform experiments using human samples. Integrated RCT from macrophages to liver and feces plays a crucial role in regulating the cholesterol homeostasis of whole body under pathophysiological condition [53-55,65,66]. Nevertheless, we did not determine the role of ADMA in macrophage-specific RCT *in vivo*. From the point in search of molecular mechanisms underlying the pathogenesis of lipid deregulation in vivo, the more informative mouse models used in the studies by Zhang et al. or Jessup et al. are required for evaluating the specific role of macrophages in ADMA-mediated deregulation in RCT under physiological condition [65,66]. To this end, further investigations describing the implications of macrophage-specific RCT in ADMA-mediated deregulation of cholesterol homeostasis *in vivo* are warranted.

In conclusion, ADMA likely has a pro-atherogenic effect based on experimental evidence showing that ADMA inhibits the oxLDL-induced activation of the LXRα pathway and downregulates the expression of ABCA1 and ABCG1, resulting in the impairment of cholesterol efflux and increased lipid accumulation in macrophage foam cells and consequently accelerating the progression of atherosclerosis. The molecular mechanisms we revealed indicate a broader biological impact of ADMA on vascular biology and suggest novel a pharmacological target for treating atherosclerosis and related cardiovascular diseases.

Conflicts of interest

The authors declare no conflict of interest.

Acknowledgments

This study was supported by grants from the Ministry of Science and Technology of Taiwan (105-2320-B-010-036, 105-2811-B-010-022, 106-2320-B-002-057-MY3, 106-2320-B-002-056, and 106-2811-B-002-146).

Author contributions

CH Chen and JF Zhao performed the experiments and analyzed the data; CP Hsu provided the research resources; YR Kou help with reviewing and editing the manuscript; TM Lu and TS Lee designed the experiments and wrote the paper.

References

[1] F. Palm, M.L. Onozato, Z. Luo, C.S. Wilcox, Dimethylarginine dimethylaminohydrolase (DDAH): expression, regulation, and function in the cardiovascular and renal systems, Am. J. Physiol. Heart Circ. Physiol. 293 (2007) H3227–3245. https://doi.org/10.1152/ajpheart.00998.2007.

[2] C.T. Tran, M.F. Fox, P. Vallance, J.M. Leiper, Chromosomal localization, DDAH2 and implication for evolutionary origins, Genomics 68 (2000) 101–105. https://doi.org/10.1006/geno.2000.6262.

[3] C.T. Tran, J.M. Leiper, P. Vallance, The DDAH/ADMA/NOS pathway, Atheroscler. Suppl. 4 (2003) 33–40. https://doi.org/10.1016/S1567-5688(03)00032-1.

[4] V. Achan, C.T.L. Tran, F. Arrigoni, G.S.J. Whitley, J.M. Leiper, P. Vallance, all-trans-Retinoic acid increases nitric oxide synthesis by endothelial cells: a role for the induction of dimethylarginine dimethylaminohydrolase, Circ. Res. 90 (2002) 764–769. https://doi.org/10.1161/01.RES.0000014450.40853.2B.

[5] H. Azumi, N. Inoue, Y. Ohashi, M. Terashima, T. Mori, H. Fujita, K. Awano, K. Kobayashi, K. Maeda, K. Hata, T. Shinke, S. Kobayashi, K. Hirata, S. Kawashima, H. Itabe, Y. Hayashi, S. Imajoh-Ohmi, H. Itoh, M. Yokoyama, Superoxide generation in directional coronary atherectomy specimens of patients with angina pectoris: important role of NAD(P)H oxidase, Arterioscler. Thromb. Vasc. Biol. 22 (2002) 1838–1844. https://doi.org/10.1161/01.ATV.0000037101.40667.62.

[6] V. Achan, H.K. Ho, C. Heeschen, M. Stuehlinger, J.J. Jang, M. Kimoto, P. Vallance, J.P. Cooke, ADMA regulates angiogenesis: genetic and metabolic evidence, Vasc. Med. 10 (2005) 7–14. https://doi.org/10.1191/1358863x05vm580

oa.

[7] R.H. Boger, S.M. Bode-Boger, A. Szuba, P.S. Tsao, J.R. Chan, O. Tangphao, T.F. Blaschke, J.P. Cooke, Asymmetric dimethylarginine (ADMA): a novel risk factor for endothelial dysfunction: its role in hypercholesterolemia, Circulation 98 (1998) 1842–1847. https://doi.org/10.1161/01.CIR.98.18.1842.

[8] Y. Chen, Y. Li, P. Zhang, J.H. Traverse, M. Hou, X. Xu, M. Kimoto, R.J. Bache, Dimethylarginine dimethylaminohydrolase and endothelial dysfunction in failing hearts, Am. J. Physiol. Heart Circ. Physiol. 289 (2005) H2212–2219. https://doi.org/10.1152/ajpheart.00224.2005.

[9] H. Dayoub, V. Achan, S. Adimoolam, J. Jacobi, M.C. Stuehlinger, B.Y. Wang, P.S. Tsao, M. Kimoto, P. Vallance, A.J. Patterson, J.P. Cooke, Dimethylarginine dimethylaminohydrolase regulates nitric oxide synthesis: genetic and physiological evidence, Circulation 108 (2003) 3042–3047. https://doi.org/10116 1/01.CIR.0000101924.04515.2E.

[10] A. Ito, P.S. Tsao, S. Adimoolam, M. Kimoto, T. Ogawa, J.P. Cooke, Novel mechanism for endothelial dysfunction: dysregulation of dimethylarginine dimethylaminohydrolase, Circulation 99 (1999) 3092–3095. https://doi.org/10.11 61/01.CIR.99.24.3092

[11] F. Arrigoni, B. Ahmetaj, J. Leiper, The biology and therapeutic potential of the DDAH/ADMA pathway, Curr. Pharm. Des. 16 (2010) 4089–5102. https://doi.org/10.2174/138161210794519246.

[12] M. Visser, W.J. Paulus, M.A. Vermeulen, M.C. Richir, M. Davids, W. Wisselink, B.A. de Mol, P.A. van Leeuwen, The role of asymmetric dimethylarginine and arginine in the failing heart and its vasculature, Eur. J. Heart Fail. 12 (2010) 1274–1281. https://doi.org/10.1093/eurjhf/hfq158.

[13] C.K. Glass, J.L. Witztum, Atherosclerosis: the road ahead, Cell 104 (2001) 503–516. https://doi.org/10.1016/S0092-8674(01)00238-0.

[14] J.A. Berliner, J.W. Heinecke, The role of oxidized lipoproteins in atherogenesis, Free Radic. Biol. Med. 20 (1996) 707–727. http://dx.doi.org/10.1155/2013/714653.

[15] A.C. Li, C.K. Glass, The macrophage foam cell as a target for therapeutic intervention, Nat. Med. 8 (2002) 1235–1242. https://doi.org /10.1038/nm1102-1235.

[16] C.W. Joyce, M.J. Amar, G. Lambert, B.L. Vaisman, B. Paigen, J. Najib-Fruchart, R.F. Hoyt Jr., E.D. Neufeld, A.T. Remaley, D.S. Fredrickson, H.B. Brewer Jr., S. Santamarina-Fojo, The ATP binding cassette transporter A1 (ABCA1) modulates the development of aortic atherosclerosis in C57BL/6 and apoE-knockout mice, Proc. Natl. Acad. Sci. U.S.A. 99 (2002) 407–412. https://doi.org/10.1073/pnas.012587699.

[17] V.V. Kunjathoor, M. Febbraio, E.A. Podrez, K.J. Moore, L. Andersson, S. Koehn, J.S. Rhee, R. Silverstein, H.F. Hoff, M.W. Freeman, Scavenger receptors class A-I/II and CD36 are the principal receptors responsible for the uptake of modified low density lipoprotein leading to lipid loading in macrophages, J. Biol. Chem. 277 (2002) 49982–49988. https://doi.org/10.1074/jbc.M209649200.

[18] R. Out, M. Hoekstra, R.B. Hildebrand, J.K. Kruit, I. Meurs, Z. Li, F. Kuipers, T.J. Van Berkel, M. Van Eck, Macrophage ABCG1 deletion disrupts lipid homeostasis in alveolar macrophages and moderately influences atherosclerotic lesion development in LDL receptor-deficient mice, Arterioscler. Thromb. Vasc. Biol. 26 (2006) 2295–2300. https://doi.org/10.1161/01.ATV.0000237629.29842.4c.

[19] S.O. Rahaman, D.J. Lennon, M. Febbraio, E.A. Podrez, S.L. Hazen, R.L. Silverstein, A CD36-dependent signaling cascade is necessary for macrophage foam cell formation, Cell Metab. 4 (2006) 211–221. https://doi.org/10.1016/j.cmet.2006.06.007.

[20] K.Y. Lu, L.C. Ching, K.H. Su, Y.B. Yu, Y.R. Kou, S.H. Hsiao, Y.C. Huang, C.Y. Chen, L.C. Cheng, C.C. Pan, T.S. Lee, Erythropoietin suppresses the formation of macrophage foam cells: role of liver X receptor α, Circulation 121 (2010) 1828–1837. https://doi.org/10.1161/CIRCULATIONAHA.109.896839.

[21] J.Y. Tsai, K.H. Su, S.K. Shyue, Y.R. Kou, Y.B. Yu, S.H. Hsiao, A.N. Chiang, Y.L. Wu, L.C. Ching, T.S. Lee, EGb761 ameliorates the formation of foam cells by regulating the expression of SR-A and ABCA1: role of haem oxygenase-1, Cardiovasc. Res. 88 (2010) 415–423. https://doi.org/10.1093/cvr/cvq226.

[22] C.Y. Chen, S.K. Shyue, L.C. Ching, K.H. Su, Y.L. Wu, Y.R. Kou, A.N. Chiang, C.C. Pan, T.S. Lee, Wogonin promotes cholesterol efflux by increasing protein phosphatase 2B-dependent dephosphorylation at ATP-binding cassette transporter-A1 in macrophages, J. Nutr. Biochem. 22 (2011) 1015–1021. https://doi.org/10.1016/j.jnutbio.2010.08.014.

[23] J.F. Zhao, L.C. Ching, Y.C. Huang, C.Y. Chen, A.N. Chiang, Y.R. Kou, S.K. Shyue, T.S. Lee, Molecular mechanism of curcumin on the suppression of cholesterol accumulation in macrophage foam cells and atherosclerosis, Mol. Nutr. Food Res. 56 (2012) 691–701. https://doi.org/10.1002/mnfr.201100735.

[24] B.F. Asztalos, M. de la Llera-Moya, G.E. Dallal, K.V. Horvath, E.J. Schaefer, G.H. Rothblat, Differential effects of HDL subpopulations on cellular ABCA1- and SR-BI- mediated cholesterol efflux, J. Lipid Res. 46 (2005) 2246–2253. https://doi.org/10.1194/jlr.M500187-JLR200.

[25] S. Lambden, P. Kelly, B. Ahmetaj-Shala, Z. Wang, B. Lee, M. Nandi, B. Torondel, M. Delahaye, L. Dowsett, S. Piper, J. Tomlinson, B. Caplin, L. Colman, O. Boruc, A. Slaviero, L. Zhao, E. Oliver, S. Khadayate, M. Singer, F. Arrigoni, J. Leiper, Dimethylarginine dimethylaminohydrolase 2 regulates nitric oxide synthesis and hemodynamics and determines outcome in polymicrobial sepsis, Arterioscler. Thromb. Vasc. Biol. 35 (2015) 1382–1392. https://doi.org/10.1161/ATVBAHA.115.305278.

[26] C.P. Hsu, J.F. Zhao, S.J. Lin, S.K. Shyue, B.C. Guo, T.M. Lu, T.S. Lee, Asymmetric dimethylarginine limits the efficacy of simvastatin activating endothelial nitric oxide synthase, J. Am. Heart Assoc. 5 (2016) e003327. https://doi.org/10.1161/JAHA.116.003327.

[27] C. Xuan, Q.W. Tian, H. Li, B.B. Zhang, G.W. He, L.M. Lun, Levels of asymmetric dimethylarginine (ADMA), an endogenous nitric oxide synthase inhibitor, and risk of coronary artery disease: A meta-analysis based on 4713 participants. Eur J Prev Cardiol. 23 (2016) 502–510. https://doi: 10.1177/2047487315586094.

[28] J.F. Zhao, H.Y. Chen, J. Wei, S.J.J. Leu, T.S. Lee, CCN family member 1 deregulates cholesterol metabolism and aggravates atherosclerosis. Acta Physiol (Oxf). 225 (2019) e13209. https://doi: 10.1111/apha.13209.

[29] X.H. Yu, Y.C. Fu, D.W. Zhang, K. Yin, C.K. Tang, Foam cells in atherosclerosis, Clin. Chim. Acta. 424 (2013) 245–252. https://doi.org/10.1016/j.cca.2013.06.006.

[30] X.H. Yu, D.W. Zhang, X.L. Zheng, C.K. Tang, Cholesterol transport system: an integrated cholesterol transport model involved in atherosclerosis, Prog. Lipid Res. 73 (2019) 65–91. https://doi.org/10.1016/j.plipres.2018.12.002.

[31] L.C Cheng, K.H. Su, Y.R. Kou, S.K. Shyue, L.C. Ching, Y.B. Yu, Y.L. Wu, C.C. Pan, T.S. Lee TS,α-Lipoic acid ameliorates foam cell formation via liver X receptor α-dependent upregulation of ATP-binding cassette transporters A1 and G1. Free Radic Biol Med. 50 (2011) 47–54. https://doi: 10.1016/j.freeradbiomed.2010.10.706.

[32] R.S. Rosenson, H.B. Brewer Jr, W.S. Davidson, Z.A. Fayad, V. Fuster, J. Goldstein, M. Hellerstein, X.C. Jiang, M.C. Phillips, D.J. Rader, A.T. Remaley, G.H. Rothblat, A.R. Tall, L. Yvan-Charvet, Cholesterol efflux and atheroprotection: advancing the concept of reverse cholesterol transport, Circulation 125 (2012) 1905–1919. https://doi.org/10.1161/CIRCULATIONAHA.111.066589.

[33] C.Y. Tsou, C.Y. Chen, J.F. Zhao, K.H. Su, H.T. Lee, S.J. Lin, S.K. Shyue, S.H. Hsiao, T.S. Lee, Activation of soluble guanylyl cyclase prevents foam cell formation and atherosclerosis, Acta Physiol. (Oxf) 210 (2014) 799–810. https://doi.org/10.1111/apha.12210.

[34] J. Wei, L.C. Ching, J.F. Zhao, S.K. Shyue, H.F. Lee, Y.R. Kou, T.S. Lee, Essential role of transient receptor potential vanilloid type 1 in evodiamine-mediated protection against atherosclerosis, Acta Physiol. (Oxf) 207 (2013) 299–307. https://doi.org/10.1111/apha.12005.

[35] M.L. Fitzgerald, Z. Mujawar, N. Tamehiro, ABC transporters, atherosclerosis and inflammation, Atherosclerosis 211 (2010) 61–70. https://doi.org/10.1016/j.atherosclerosis.2010.01.011.

[36] D.A. Chistiakov, Y.V. Bobryshev, A.N. Orekhov, Macrophage-mediated cholesterol handling in atherosclerosis, J. Cell. Mol. Med. 20 (2016) 17–28. https://doi.org/10.1111/jcmm.12689.

[37] C. Weber, H. Noels, Atherosclerosis: current pathogenesis and therapeutic options, Nat. Med. 17 (2011) 1410–1422. https://doi.org/10.1038/nm.2538.

[38] S. Abhary, K.P. Burdon, A. Kuot, S. Javadiyan, M.J. Whiting, N. Kasmeridis, N. Petrovsky, J.E. Craig, Sequence variation in DDAH1 and DDAH2 genes is strongly and additively associated with serum ADMA concentrations in individuals with type 2 diabetes, PLoS One 5 (2010) e9462. https://doi.org/10.1371/journal.pone.0009462.

[39] M. Anderssohn, E. Schwedhelm, N. Lüneburg, R.S. Vasan, R.H. Böger, Asymmetric dimethylarginine as a mediator of vascular dysfunction and a marker of cardiovascular disease and mortality: an intriguing interaction with diabetes mellitus, Diab. Vasc. Dis. Res. 7 (2010) 105–118. https://doi.org/ 10.1177/1479164110366053.

[40] R.H. Böger, C. Zoccali, ADMA: a novel risk factor that explains excess cardiovascular event rate in patients with end-stage renal disease, Atheroscler. Suppl. 4 (2003) 3–28. https://doi.org/10.1016/S1567-5688(03)00030-8.

[41] M. Chen, Y. Li, T. Yang, Y. Wang, Y. Bai, X. Xie, ADMA induces monocyte adhesion via activation of chemokine receptors in cultured THP-1 cells, Cytokine 43 (2008) 149-159. https:// doi: 10.1016/j.cyto.2008.05.001.

[42] Z.D. Zhu, Z. Yu, X. Zhang, Y.J. Wang, D.H. Wang, Effect of asymmetric dimethylarginine on MIF expression and TNF-α and IL-8 secretion in THP-1 monocytes-derived macrophages, Nan Fang Yi Ke Da Xue Xue Bao 31 (2011) 1–4. https://doi.org/CNKI:44-1627/R.20101230.1122.000.

[43] P. Zahradka. Inhibition of NADPH oxidase by vaspin may prevent progression of atherosclerosis. Acta Physiol (Oxf). 209 (201) 195–198. https://doi: 10.1111/apha.12166.N. Panth, K.R. Paudel, K. Parajuli, Reactive oxygen species:

a key hallmark of cardiovascular disease, Adv. Med. 2016 (2016) 9152732. https://doi.org/ 10.1155/2016/9152732.

[44] A. Sirker, M. Zhang, A.M. Shah, NADPH oxidases in cardiovascular disease: insights from in vivo models and clinical studies, Basic Res. Cardiol. 106 (2011) 735–747. https://doi.org/10.1007/s00395-011-0190-z.

[45] S.H. Juan, T.S. Lee, K.W. Tseng, J.Y. Liou, S.K. Shyue, K.K. Wu, L.Y. Chau, Adenovirus-mediated heme oxygenase-1 gene transfer inhibits the development of atherosclerosis in apolipoprotein E-deficient mice, Circulation 104 (2001) 1519–1525. https://doi.org/10.1161/hc3801.095663.

[46] I. Jialal, S. Devaraj, Antioxidants and atherosclerosis: don't throw out the baby with the bath water, Circulation 107 (2003) 926–928. https://doi.org/ 10.1161/01.CIR.0000048966.26216.4C.

[47] Y.L. Tain, Y.H. Kao, C.S. Hsieh, C.C. Chen, J.M. Sheen, I.C. I.C. Lin, L.T. Huang, Melatonin blocks oxidative stress-induced increased asymmetric dimethylarginine. Free Radic Biol Med. 49 (2010) 1088–1098. https://doi:10.1016/j.freeradbiomed.2010.06.029.

[48] S. Kumar, X. Sun, S.K. Noonepalle, Q. Lu, E. Zemskov, T. Wang, S. Aggarwal, C. Gross, S. Sharma, A.A. Desai, Y. Hou, S. Dasarathy, N. Qu, V. Reddy, S.G. Lee, M. Cherian-Shaw, J.X. Yuan, J.D. Catravas, R. Rafikov, J.G.N. Garcia, S.M. Black, Hyper-activation of pp60Src limits nitric oxide signaling by increasing asymmetric dimethylarginine levels during acute lung injury. Free Radic Biol Med. 102 (2017) 217–228. https://doi: 10.1016/j.freeradbiomed.2016.11.008.

[49] J. Jacobi, R. Maas, A.J. Cardounel, M. Arend, A.J. Pope, N. Cordasic, J. Heusinger-Ribeiro, D. Atzler, J. Strobel, E. Schwedhelm, R.H. Böger, K.F. Hilgers, Dimethylarginine dimethylaminohydrolase overexpression ameliorates

atherosclerosis in apolipoprotein E-deficient mice by lowering asymmetric dimethylarginine, Am. J. Pathol. 176 (2010) 2559–2570. https://doi.org/10.2353/ajpath.2010.090614.

[50] Y. Lu, Y.P. Jia, Quercetin upregulates ABCA1 expression through liver X receptor alpha signaling pathway in THP-1 macrophages, Eur. Rev. Med. Pharmacol. Sci. 20 (2016) 3945–3952.

[51] A.Z. Ma, Q. Zhang, Z.Y. Song, TNFa alter cholesterol metabolism in human macrophages via PKC-θ-dependent pathway, BMC Biochem. 14 (2013) 20. https://doi.org/10.1186/1471-2091-14-20.

[52] R. Zhu, Z. Ou, X. Ruan, J. Gong, Role of liver X receptors in cholesterol efflux and inflammatory signaling (review), Mol. Med. Rep. 5 (2012) 895–900. https://doi.org/10.3892/mmr.2012.758.

[53] Y.V. Bobryshev, E.A. Ivanova, D.A. Chistiakov, N.G. Nikiforov, A.N. Orekhov, Macrophages and their role in atherosclerosis: pathophysiology and transcriptome analysis, Biomed Res. Int. 2016 (2016) 9582430. https://doi.org/10.1155/2016/9582430.

[54] M. Baranowski, P. Zabielsk, A.U. Błachnio-Zabielska, D. Harasiuk, J. Górski, LXR activation prevents exhaustive exercise-induced hypoglycaemia and spares muscle glycogen but does not enhance running endurance in untrained rats. Acta Physiol (Oxf). 201 (2011) 373–379. https://doi: 10.1111/j.1748-1716.2010.02199.x..

[55] C. Andersson, M.M. Zaman, A.B. Jones, S.D. Freedman, Alterations in immune response and PPAR/LXR regulation in cystic fibrosis macrophages, J. Cyst. Fibros. 7 (2008) 68–78. https://doi.org/10.1016/j.jcf.2007.05.004.

[56] I.G. Schulman, Liver X receptors link lipid metabolism and inflammation, FEBS

Lett 591 (2017) 2978–2991. https://doi.org/10.1002/1873-3468.12702.

[57] M.V. Cannon, W.H. van Gilst, R.A. de Boer, Emerging role of liver X receptors in cardiac pathophysiology and heart failure, Basic Res. Cardiol. 111 (2016) 3. https://doi.org/10.1007/s00395-015-0520-7.

[58] M.B. Fessler, The challenges and promise of targeting the Liver X Receptors for treatment of inflammatory disease, Pharmacol. Ther. 181 (2018) 1–12. https://doi.org/10.1016/j.pharmthera.2017.07.010.

[59] N. Zelcer, P. Tontonoz, Liver X receptors as integrators of metabolic and inflammatory signaling, J. Clin. Invest. 116 (2006) 607–614. https://doi.org/ 10.1172/JCI27883.

[60] D. Han, X. Li, S. Li, T. Su, L. Fan, W.S. Fan, H.Y. Qiao, J.W. Chen, M.M. Fan, X.J. Li, Y.B.Wang, S. Ma, Y. Qiu, Z.H. Tian, F. Cao, Reduced silent information regulator 1 signaling exacerbates sepsis-induced myocardial injury and mitigates the protective effect of a liver X receptor agonist. Free Radic Biol Med. 113 (2017) 291–303. https://doi: 10.1016/j.freeradbiomed.2017.10.005.

[61] G. Serviddio, F. Bellanti, G. Vendemiale, Oxysterols in the orchestra of liver cell metabolism. Free Radic Biol Med. Suppl 1 (2014) S6. https://doi: 10.1016/j.freeradbiomed.2014.10.838.

[62] Y. Gong, Y. Yang, Q. Wu, G. Gao, Y. Liu, Y. Xiong, C. Huang, S. Wu, Activation of LXRα improves cardiac remodeling induced by pulmonary artery hypertension in rats, Sci. Rep. 7 (2017) 6169. https://doi.org/ 10.1038/s41598-01 7-04640-6.

[63] C.P. Hsu, C.H. Lin, C.Y. Kuo, Endothelial-cell inflammation and damage by reactive oxygen species are prevented by propofol via ABCA1-mediated cholesterol efflux, Int. J. Med. Sci. 15 (2018) 978–985. https://doi.org/

10.7150/ijms.24659.

[64] G. Serviddio, F. Bellanti, G. Vendemiale, Free radical biology for medicine: learning from nonalcoholic fatty liver disease. Free Radic Biol Med. 65 (2013) 952–968. https://doi: 10.1016/j.freeradbiomed.2013.08.174.

[65] Y. Zhang, I. Zanotti, M.P. Reilly, J.M. Glick, G.H. Rothblat, D.J. Rader, Overexpression of apolipoprotein A-I promotes reverse transport of cholesterol from macrophages to feces in vivo. Circulation. 108 (2003) 661–663. https://doi.org/ 10.1161/01.CIR.0000086981.09834.E0

[66] M. Kockx, W. Jessup, L. Kritharides, Measurement of macrophage-specific in vivo reverse cholesterol transport in mice. Methods Mol Biol.1583 (2017) 287-298. https://doi:10.1007/978-1-4939-6875-6_21.

Figure Legends

***Fig. 1*. Effect of oxLDL on the macrophage ADMA/DDAH-2 system.** (A) Aortas were collected from 5-month-old *apoE*$^{-/-}$ mice. Immunostaining was performed with normal rabbit IgG, anti-DDAH-1, anti-DDAH-2, or anti-F4/80 antibody, a macrophage marker. Cell nuclei were stained with hematoxylin. Bar = 50 μm. Murine J774.A1 macrophages or human THP-1-derived macrophages were treated with indicated concentrations of oxLDL for 24 h. (B and D) Western blot analysis of DDAH-1, DDAH-2, and α-tubulin. (C and E) Intracellular ADMA was measured by ELISA assays. Data are the mean ± SEM from five independent experiments. **P* < 0.05 vs. the vehicle group.

***Fig. 2*. Effect of ADMA on the oxLDL-induced lipid accumulation**. Murine J774.A1 macrophages or human THP-1-derived macrophages were treated with indicated concentrations of ADMA in the presence of oxLDL (50 μg/ml) for 24 h. (A) Intracellular cholesterol and triglycerides were extracted and measured using an enzymatic method. Data are the mean ± SEM from five independent experiments. (B) Representative microscopy images of oil red O staining. (C and E) Cells were treated with indicated concentrations of ADMA with or without Dil-oxLDL (2 μg/ml). Fold change in lipid accumulation in macrophages by fluorescent assay. (D and F) Representative fluorescent microscopy images of lipid accumulation. Scale bar = 10 μm. **P* < 0.05 vs. the vehicle group; $^{\#}$*P* < 0.05 vs. the oxLDL alone group.

***Fig. 3*. Effect of ADMA on oxLDL internalization and SR expression.** (A and D) Murine J774A.1 macrophages or human THP-1-derived macrophages were treated with vehicle or ADMA (0.5 μM) for 24 h then incubated with 2 μg/ml Dil-oxLDL at 4 °C for 4 h. Fold change in lipid binding on surface of macrophages by fluorescent

assay. (B, C, E and F) Western blot analysis of SR-A, CD36, and α-tubulin. Data are the mean ± SEM from five independent experiments. *$P < 0.05$ vs. the vehicle group.

Fig. 4. **The implication of ADMA in cholesterol efflux and expression of cholesterol transporters.** (A, B, D and E) Murine J774A.1 macrophages or human THP-1-derived macrophages were treated with indicated treatments; apoAI- or HDL-dependent cholesterol efflux was determined by fluorescent assay. (C and F) Macrophages were incubated with indicated treatments for 24 h. Western blot analysis of ABCA1, ABCG1, SR-BI, and α-tubulin. Data are the mean ± SEM from five independent experiments. *$P < 0.05$ vs. the vehicle group; $^{\#}P < 0.05$ vs. the oxLDL alone group.

Fig. 5. **Effect of ADMA on LXRα activation.** (A) J774A.1 macrophages were incubated with the indicated treatments for 6 h. Real-time PCR analysis of mRNA levels of ABCA1, ABCG1, or GAPDH. (B) Western blot analysis of nuclear LXRα and Histone H1. (C) J774A.1 macrophages were transfected with pM-GAL-hLXRα with a GAL4-SEAP reporter for 24 h and then incubated with indicated reagents for another 24 h. The SEAP activity in the culture media was determined. Data are the mean ± SEM from five independent experiments. *$P < 0.05$ vs. the vehicle group; $^{\#}P < 0.05$ vs. the oxLDL alone group.

Fig. 6. **Effect of DDAH-2 overexpression on the ADMA-mediated deregulation of cholesterol metabolism.** (A) J774.A1 cells were infected with adenovirus (Ad) Ad-DDAH-2 (12.5-50 MOI) for 24 h. Western blot analysis of DDAH-2 and α-tubulin. (B and C) J774.A1 cells were infected with Ad-vector (Ad-null) or Ad-DDAH-2 (50 MOI) for 24 h, and then treated with indicated treatments for 12 h; apoAI- or HDL-dependent cholesterol efflux was determined by fluorescent assay. (D) Fold change in lipid accumulation in macrophages by fluorescent assay after

Dil-oxLDL treatment for 24 h. (E) Representative fluorescent microscopy images of lipid accumulation. Scale bar = 20 μm. Data are the mean ± SEM from five independent experiments. $^{*}P < 0.05$ vs. the vehicle group; $^{\#}P < 0.05$ vs. the oxLDL alone group; $^{\&}P < 0.05$ vs. the ADMA+oxLDL group.

Fig. 7. **Effect of ADMA on the activation of the NOX-ROS pathway**. J77A1.A1 macrophages were treated with ADMA (0.5 μg/ml) for the indicated times. (A) $NADP^{+}$/NADPH assay, the intensity of (B) red fluorescent DHE, and (C) green fluorescent DCF, were analyzed. (D and E) Representative fluorescent microscopy images of ROS. Scale bar = 20 μm. Data are the mean ± SEM from five independent experiments. $^{*}P < 0.05$ vs vehicle.

Fig. 8. **Effects of inhibition of NOX-ROS signaling on ADMA-induced ROS production and deregulation of cholesterol efflux**. (A and B) J774.A1 cells were pretreated with or without an NOX inhibitor (apocynin; APO, 50 μM) or a ROS scavenger (N-acetylcysteine; NAC, 10 mM) for 2 h and then ADMA (0.5 μg/ml) for 15 min. Intracellular levels of ROS were assessed. (C and D) J774.A1 macrophages were pretreated with or without APO or NAC for 2 h and then indicated treatments. ApoAI- or HDL-dependent cholesterol efflux was evaluated. (E) Fold change in lipid accumulation in macrophages by fluorescent assay (F) Representative fluorescent microscopy images of lipid accumulation. J774.A1 cells were transfected with or without NOX2 siRNA for 24 h, followed by indicated treatments. (G and H) Representative fluorescent images of ROS; (I) Intracellular lipid accumulation and (J) Representative fluorescent images of lipid accumulation. Scale bar = 20 μm. $^{*}P < 0.05$ vs. the vehicle group; $^{\#}P < 0.05$ vs. the oxLDL alone group; $^{\&}P < 0.05$ vs. the ADMA+ oxLDL group.

Fig. 9. **Effects of chronic treatment with ADMA on RCT and atherosclerosis in *apoE*$^{-/-}$ mice**. Male apoE$^{-/-}$ mice received a daily administration of ADMA (5 mg/kg, n=10) or saline (vehicle control, n=10) for 4 weeks. (A) Quantitation of atherosclerotic lesions in the aortic roots of vehicle-treated or ADMA-treated apoE$^{-/-}$ mice. (B) Serum levels of cholesterol, non-high-density lipoprotein cholesterol (non-HDL-c), HDL cholesterol (HDL-c) and triglycerides. (C) Western blotting analysis of aortic levels of LXRα, ABCA1, ABCG1, SR-BI, SR-A, CD36, and α-tubulin. (D) The reverse cholesterol efflux efficacy of serum. (E) Serum levels of tumor necrosis factor α (TNF-α), interleukin-1β (IL-1β), IL-6, monocyte chemotactic protein 1 (MCP-1), and macrophage inflammatory protein 2 (MIP-2). Data for each group are the mean ± SEM from 10 animals. *, $P < 0.05$ vs. vehicle-treated mice.

Fig. 10. **Schematic illustration of the proposed mechanism underlying the ADMA-mediated deregulation of cholesterol metabolism in macrophages.** As shown, challenge with ADMA elicits the activation of the NOX-ROS pathway, which in turn reduces LXRα activity and downregulates the expression of ABCA1 and ABCG1, leading to the impairment of cholesterol efflux and ultimately increasing lipid accumulation in macrophages.

Figure 10

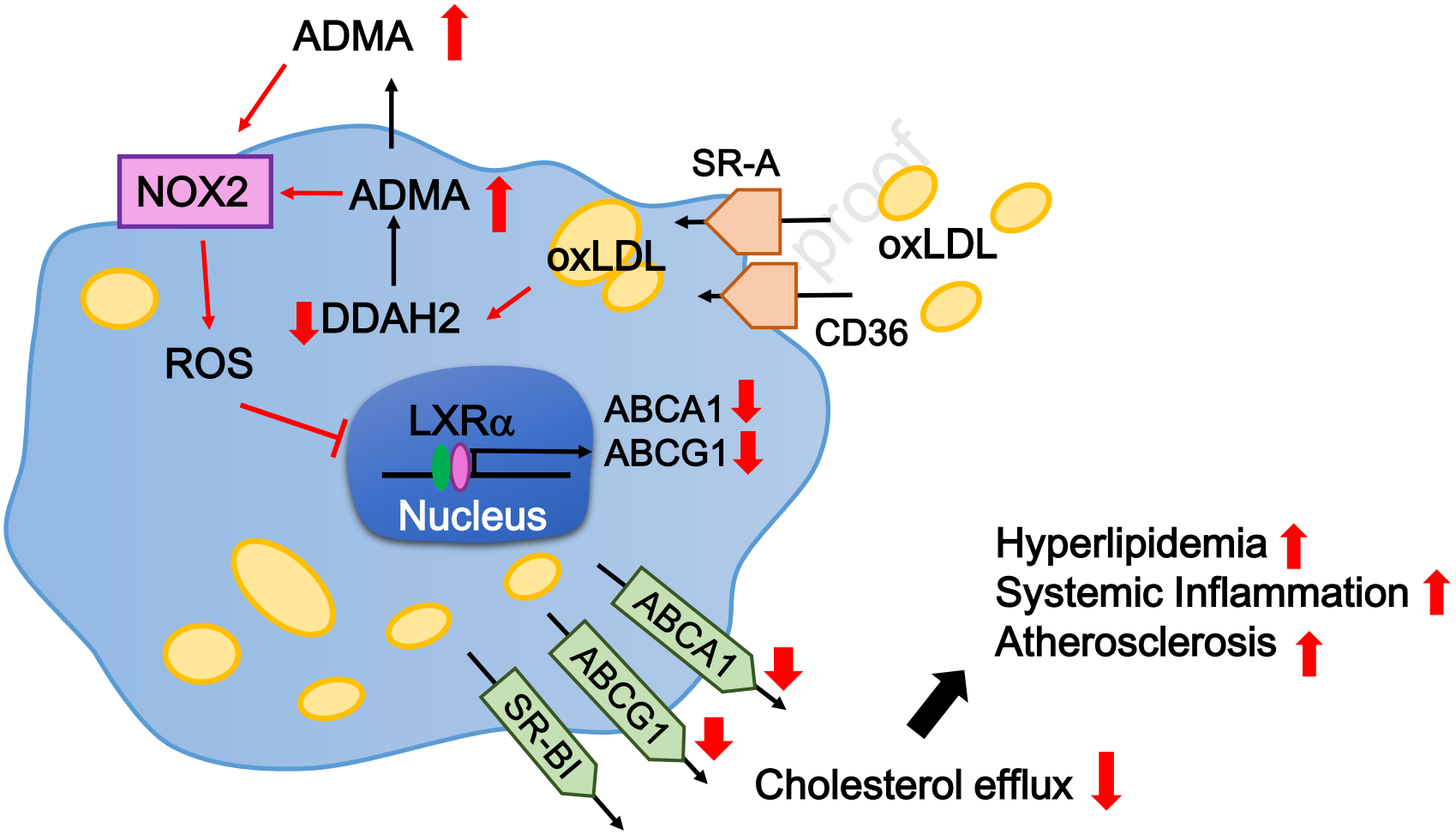

Figure 1

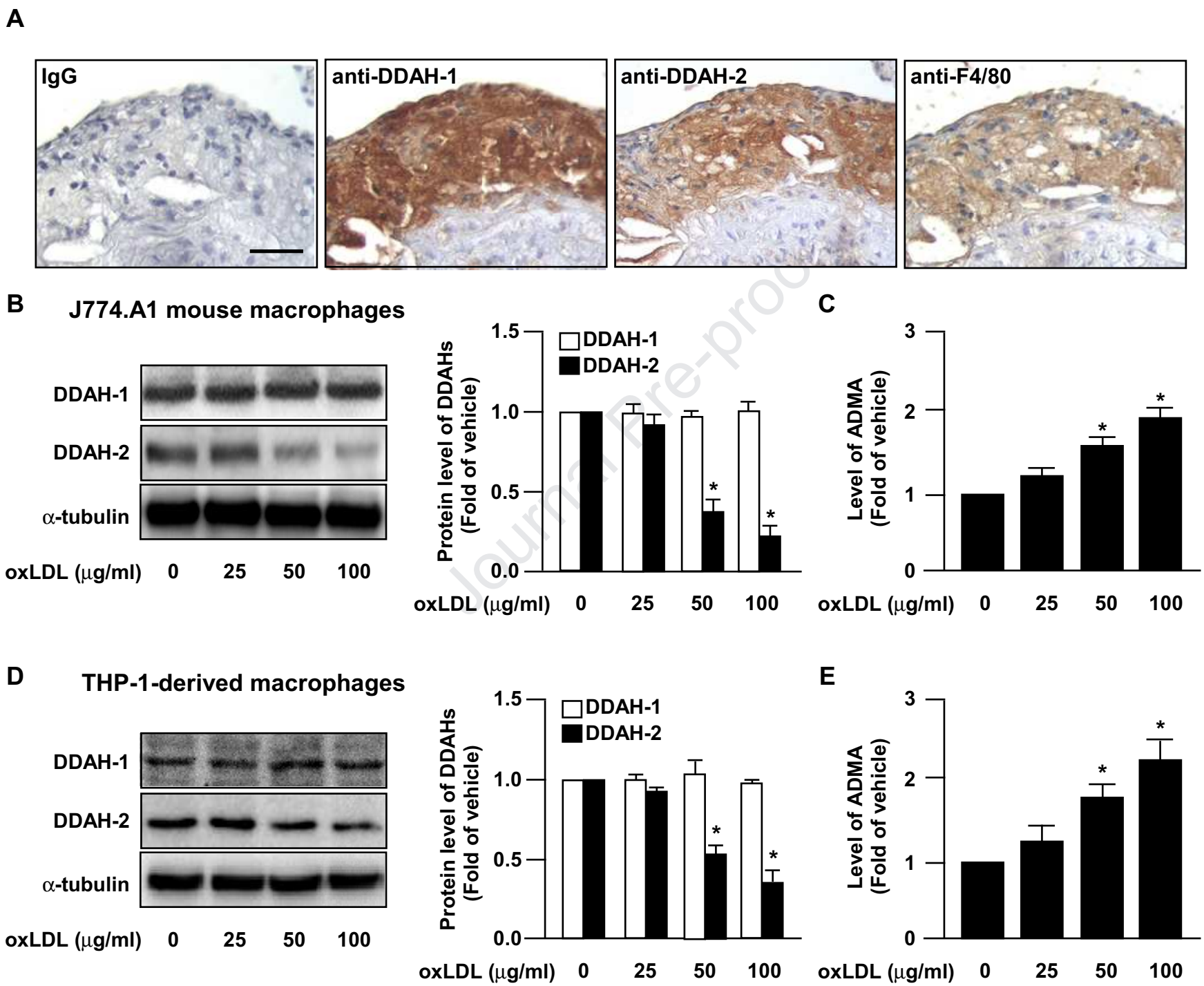

Figure 2

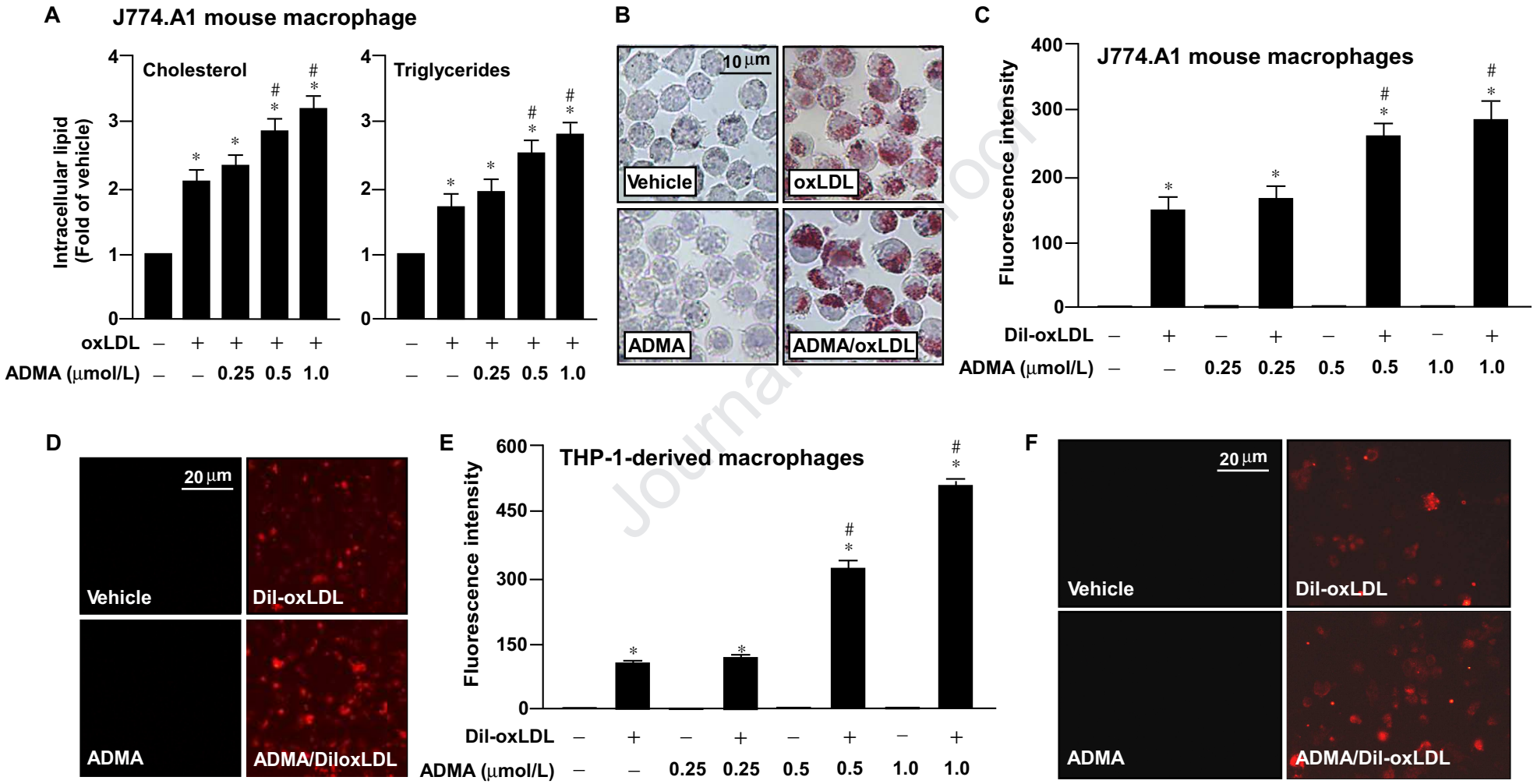
A
J774.A1 mouse macrophage
Cholesterol
Triglycerides
Intracellular lipid (Fold of vehicle)
oxLDL
ADMA (μmol/L)
0.25
0.5
1.0
B
10 μm
Vehicle
oxLDL
ADMA
ADMA/oxLDL
C
J774.A1 mouse macrophages
Fluorescence intensity
Dil-oxLDL
ADMA (μmol/L)
D
20 μm
Vehicle
Dil-oxLDL
ADMA
ADMA/DiloxLDL
E
THP-1-derived macrophages
Fluorescence intensity
Dil-oxLDL
ADMA (μmol/L)
F
20 μm
Vehicle
Dil-oxLDL
ADMA
ADMA/Dil-oxLDL

Figure 3

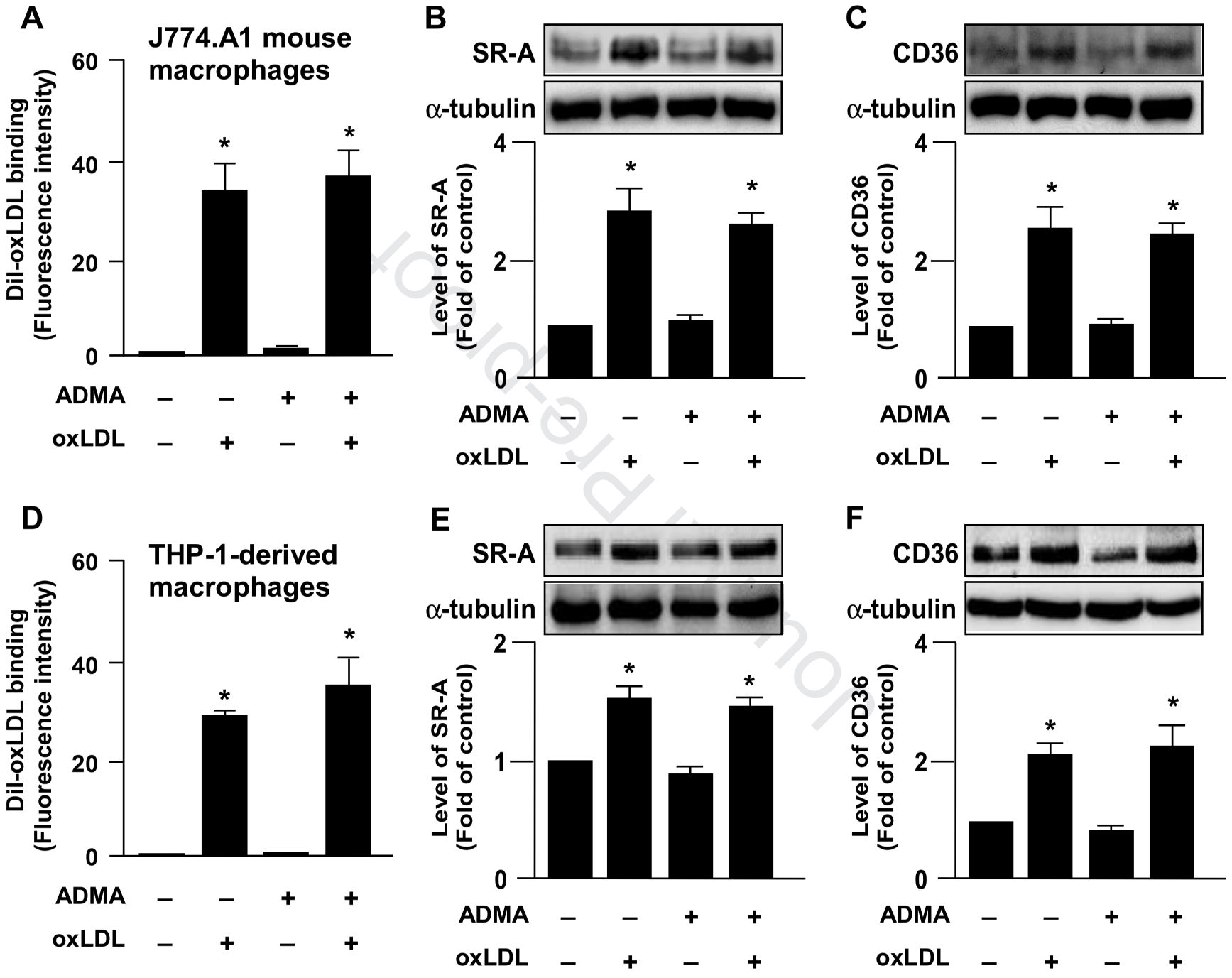

Figure 4

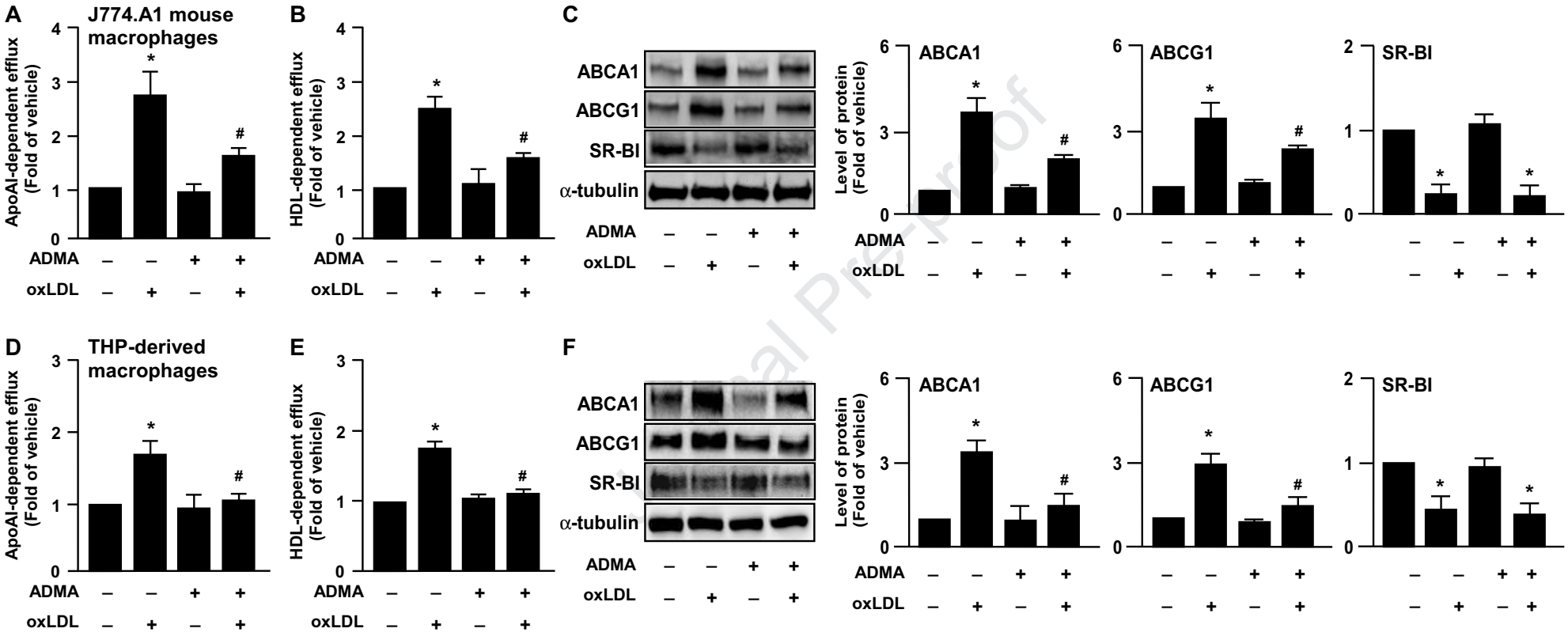

Figure 5

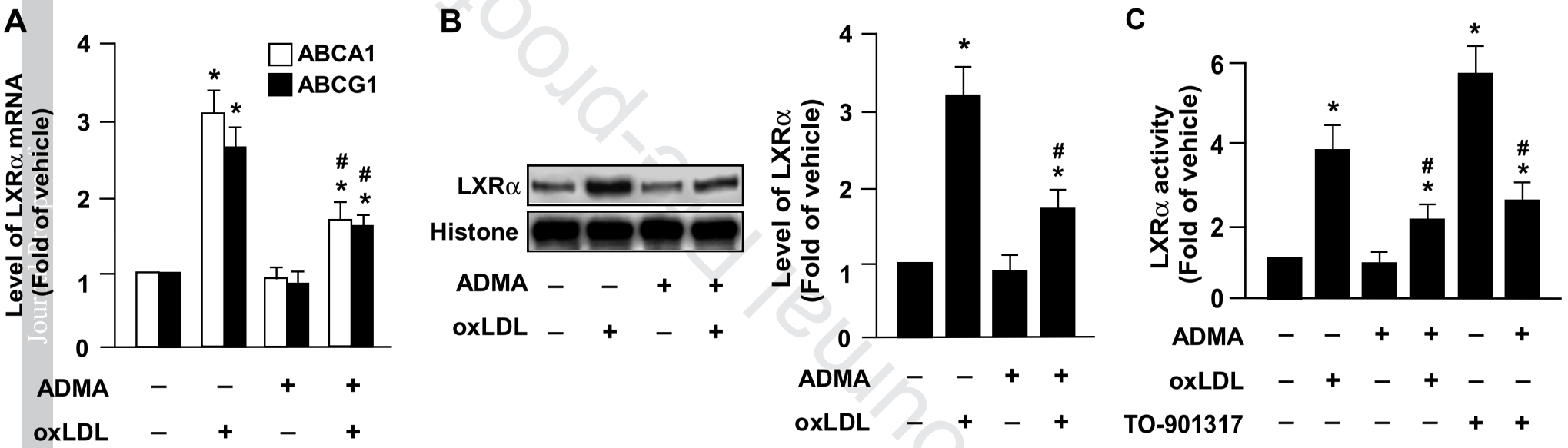

Figure 6

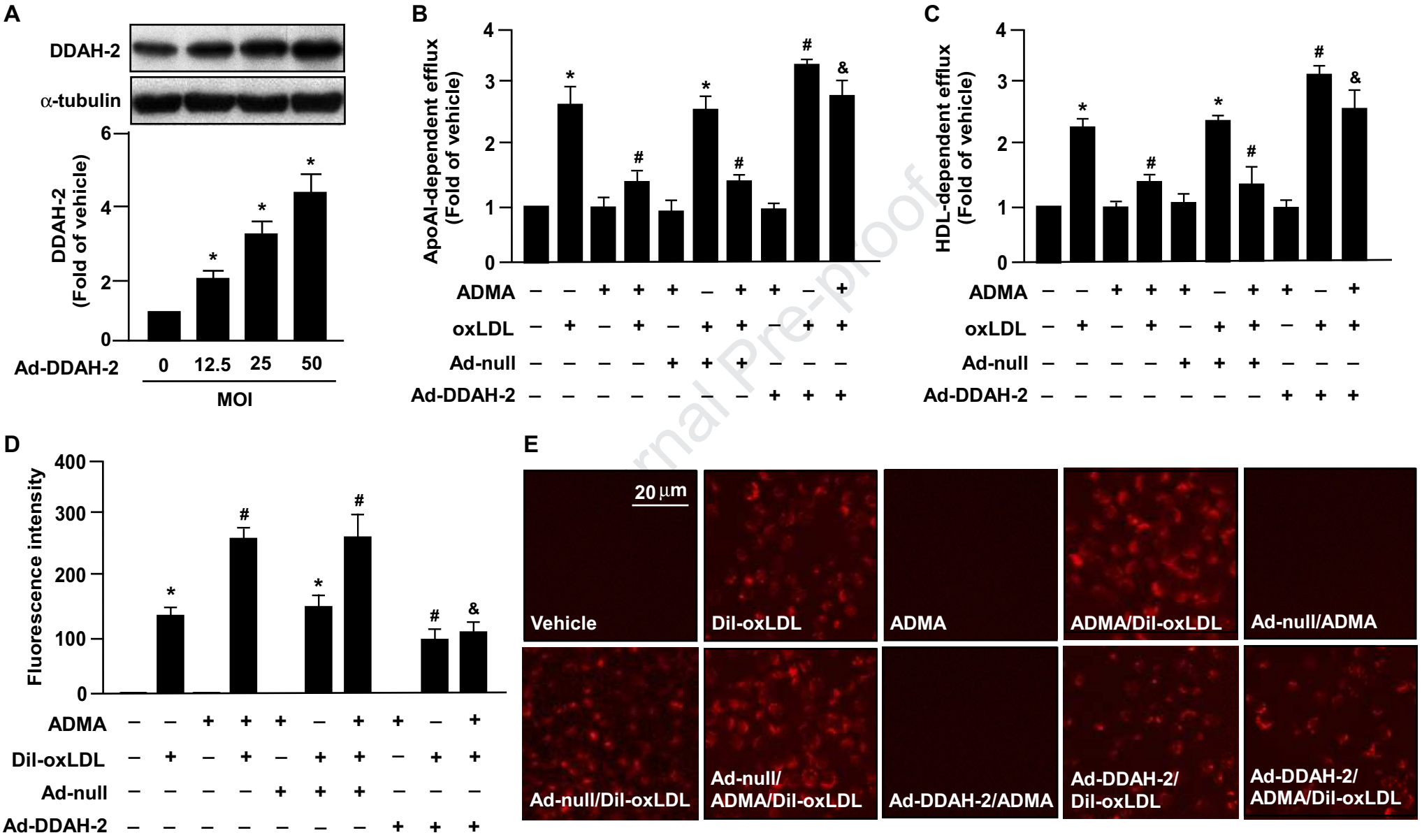
A
DDAH-2
α-tubulin
DDAH-2 (Fold of vehicle)
Ad-DDAH-2
0
12.5
25
50
MOI
B
ApoAI-dependent efflux (Fold of vehicle)
ADMA
oxLDL
Ad-null
Ad-DDAH-2
C
HDL-dependent efflux (Fold of vehicle)
ADMA
oxLDL
Ad-null
Ad-DDAH-2
D
Fluorescence intensity
ADMA
Dil-oxLDL
Ad-null
Ad-DDAH-2
E
20 μm
Vehicle
Dil-oxLDL
ADMA
ADMA/Dil-oxLDL
Ad-null/ADMA
Ad-null/Dil-oxLDL
Ad-null/ ADMA/Dil-oxLDL
Ad-DDAH-2/ADMA
Ad-DDAH-2/ Dil-oxLDL
Ad-DDAH-2/ ADMA/Dil-oxLDL

Figure 7

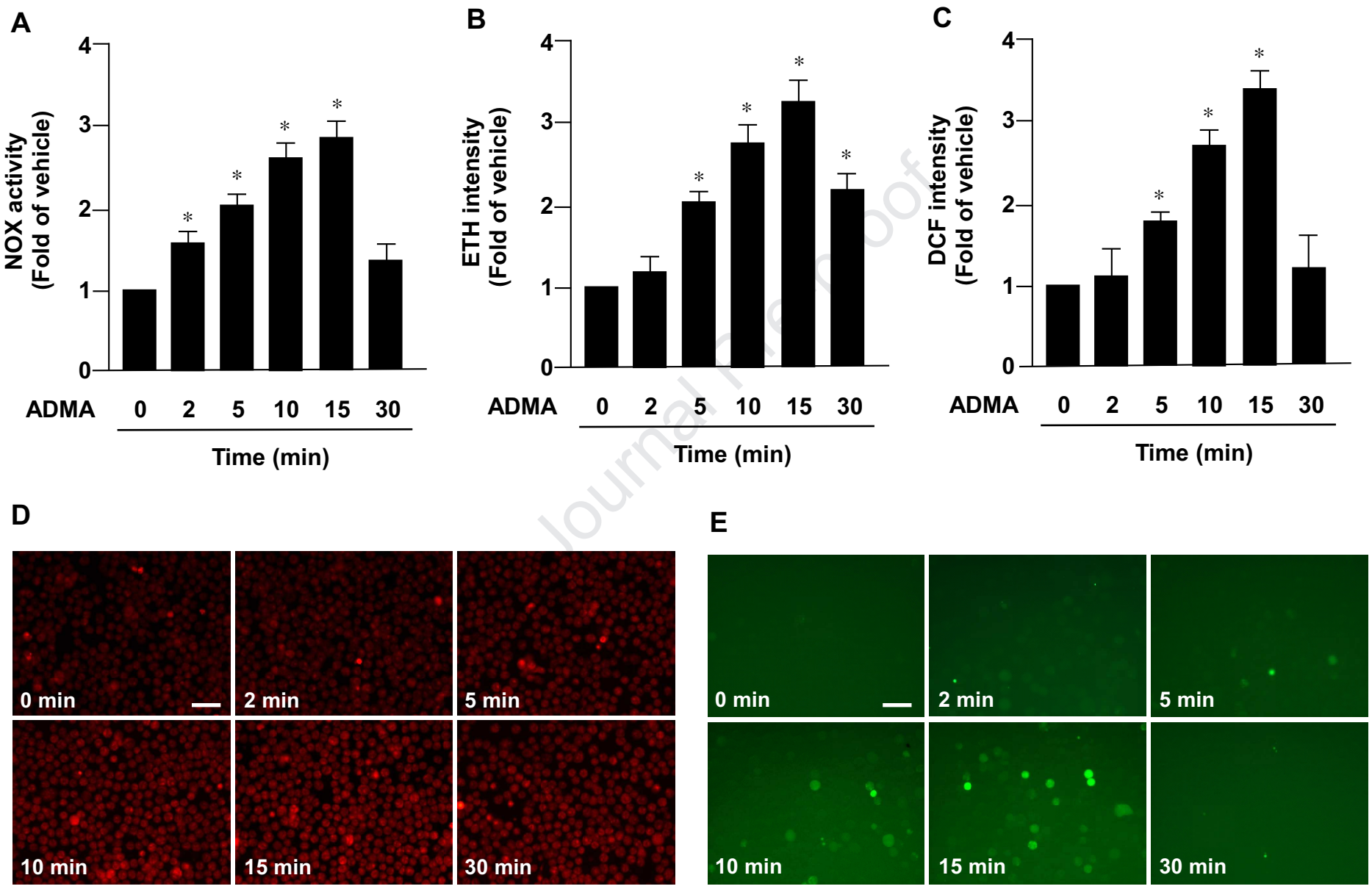

Figure 8

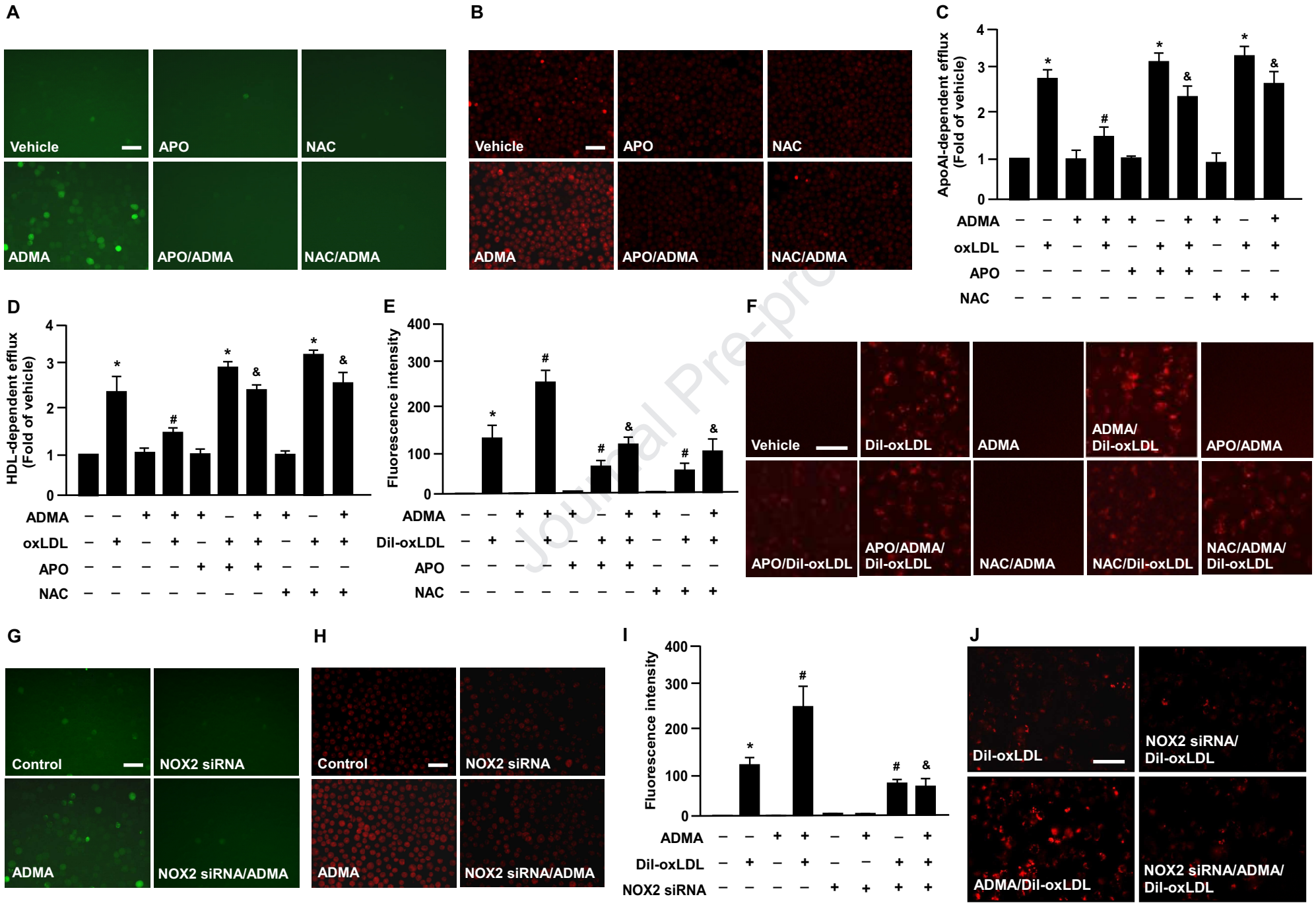

Figure 9

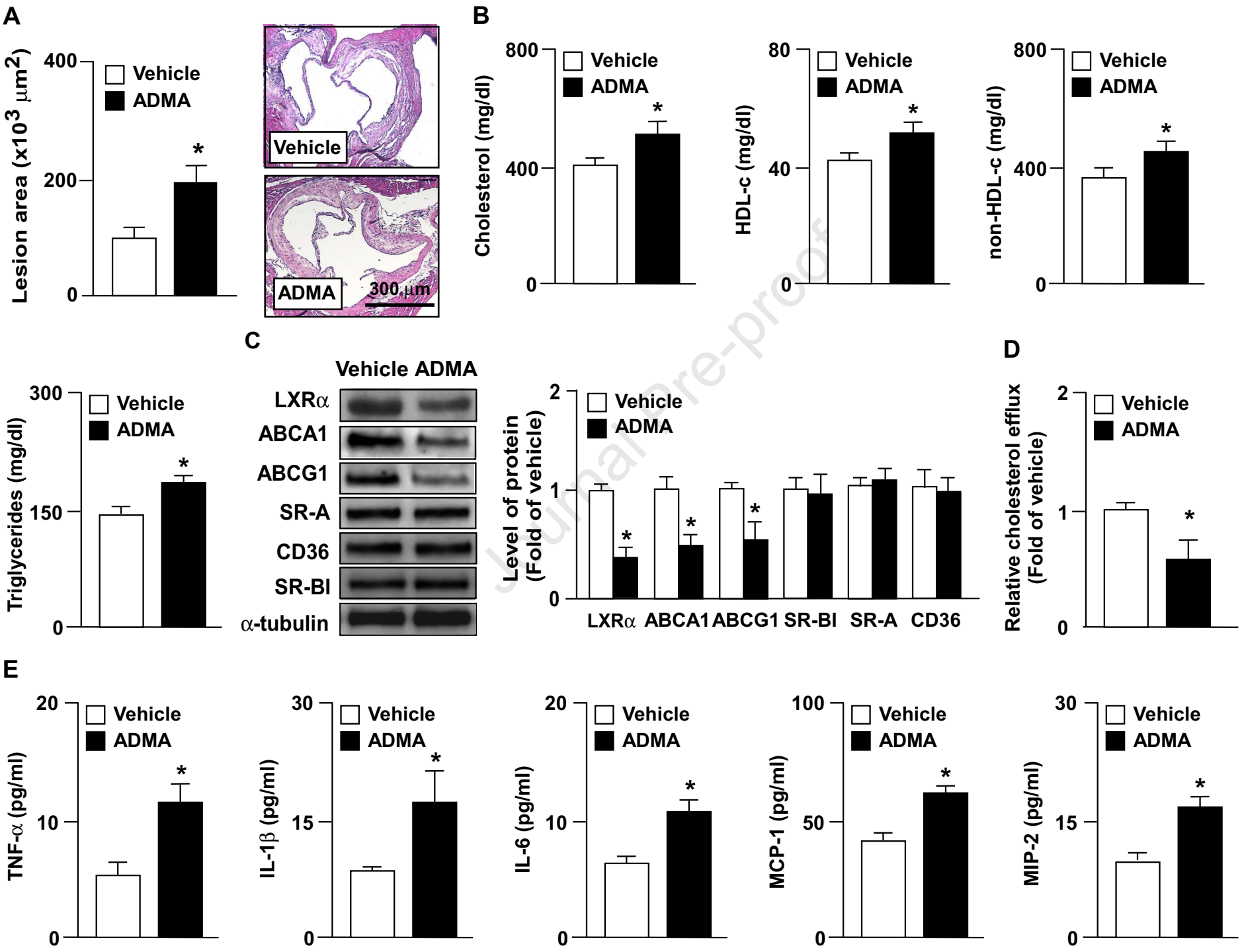

Highlights

1. ADMA exacerbates oxLDL-induced lipid accumulation in macrophage foam cells.

2. ADMA impairs cholesterol efflux by decreasing the expression and activity of LXRα.

3. DDAH-2 overexpression prevents the detrimental effects of ADMA on cholesterol efflux.

4. ADMA activates the NOX/ROS signaling pathway.

5. ADMA exacerbates hyperlipidemia, inflammation and atherosclerosis in apoE$^{-/-}$ mice.